AD-A149 845 SIDE MOMENT EXERTED BY A TWO-COMPONENT LIQUID PAYLOAD 1/1
ON A SPINNING PROJECTILE(U) ARMY BALLISTIC RESEARCH LAB
ABERDEEN PROVING GROUND MD C H MURPHY DEC 84
UNCLASSIFIED BRL-TR-2624 SBI-AD-F300 556 F/G 19/1 NL

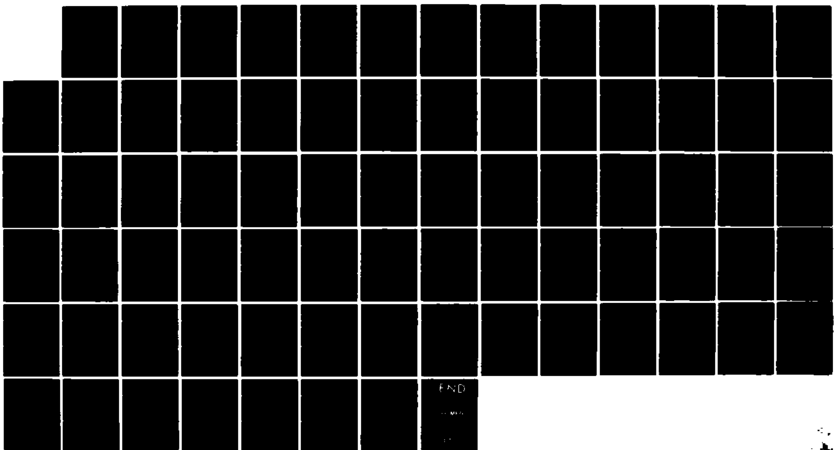

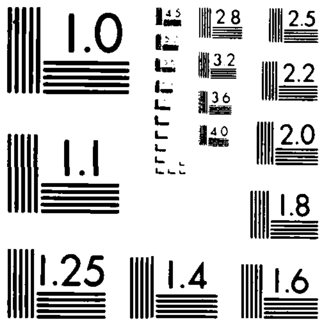

MICROCOPY RESOLUTION TEST CHART
NATIONAL BUREAU OF STANDARDS-1963-A

AD-A149 845

AD

BRL

TECHNICAL REPORT BRL-TR-2624

SIDE MOMENT EXERTED BY A TWO-COMPONENT LIQUID PAYLOAD ON A SPINNING PROJECTILE

Charles H. Murphy

December 1984

US ARMY BALLISTIC RESEARCH LABORATORY
ABERDEEN PROVING GROUND, MARYLAND

85 02 ... 111

UNCLASSIFIED

SECURITY CLASSIFICATION OF THIS PAGE (When Data Entered)

REPORT DOCUMENTATION PAGE

READ INSTRUCTIONS BEFORE COMPLETING FORM

1. REPORT NUMBER: TECHNICAL REPORT BRL-TR-2624
2. GOVT ACCESSION NO.: AD-A149 845
3. RECIPIENT'S CATALOG NUMBER:
4. TITLE (and Subtitle): SIDE MOMENT EXERTED BY A TWO-COMPONENT LIQUID PAYLOAD ON A SPINNING PROJECTILE
5. TYPE OF REPORT & PERIOD COVERED: Final
6. PERFORMING ORG. REPORT NUMBER:
7. AUTHOR(s): Charles H. Murphy
8. CONTRACT OR GRANT NUMBER(s):
9. PERFORMING ORGANIZATION NAME AND ADDRESS: US Army Ballistic Research Laboratory, ATTN: AMXBR-LFD, Aberdeen Proving Ground, Maryland 21005-5066
10. PROGRAM ELEMENT, PROJECT, TASK AREA & WORK UNIT NUMBERS: RDT&E 1L161102AH43
11. CONTROLLING OFFICE NAME AND ADDRESS: US Army Ballistic Research Laboratory, ATTN: AMXBR-OD-ST, Aberdeen Proving Ground, Maryland 21005-5066
12. REPORT DATE: December 1984
13. NUMBER OF PAGES: 79
14. MONITORING AGENCY NAME & ADDRESS (if different from Controlling Office):
15. SECURITY CLASS. (of this report): UNCLASSIFIED
15a. DECLASSIFICATION DOWNGRADING SCHEDULE:

16. DISTRIBUTION STATEMENT (of this Report)

Approved for public release; distribution unlimited.

17. DISTRIBUTION STATEMENT (of the abstract entered in Block 20, if different from Report)

18. SUPPLEMENTARY NOTES

19. KEY WORDS (Continue on reverse side if necessary and identify by block number)

Eigenfrequency
Gyroscope
Liquid Moment
Spinning Projectile
Two-Liquid Payload

20. ABSTRACT (Continue on reverse side if necessary and identify by block number) (bja)

A linear boundary layer theory is derived for two liquids in a cylindrical cavity in a coning and spinning projectile. Predicted eigenfrequencies agree well with available experimental results. Side moment coefficients are computed for various cases. It is shown that significant increases in the single-liquid side moment can be caused by the addition of a small amount of heavier liquid and for certain locations of the liquid interface, pairs of eigenfrequencies can coalesce.

DD FORM 1 JAN 73 1473 EDITION OF 1 NOV 65 IS OBSOLETE

UNCLASSIFIED

SECURITY CLASSIFICATION OF THIS PAGE (When Data Entered)

TABLE OF CONTENTS

LIST OF ILLUSTRATIONS

LIST OF ILLUSTRATIONS (cont'd)

LIST OF TABLES

I. INTRODUCTION

The prediction of the complete moment exerted by a spinning liquid payload on a spinning and coning projectile has been a problem of considerable interest to the Army for some time. For a fully spinning liquid, the linear side moment was first computed by Stewartson[1] for an inviscid payload by use of eigenfrequencies determined by the fineness ratio of the cylindrical container. Wedemeyer[2] introduced boundary layers on the walls of the container and was able to determine viscous corrections for Stewartson's eigenfrequencies, which could then be used in Stewartson's side moment calculation. Murphy[3] then completed the linear boundary layer theory by including all pressure and wall shear contributions to the liquid-induced side moment. The Stewartson-Wedemeyer eigenvalue calculations have been improved for low Reynolds numbers by Kitchens *et al.*[4] through the replacement of the cylindrical wall boundary approximation by a linearized Navier-Stokes approach. Next, Gerber *et al.*[5-6] extended this linearized NS technique to compute better side moment coefficients for Reynolds numbers less than 10,000. Finally, the roll moment for a fully spun-up liquid was computed by Murphy.[7-8]

---

1. *K. Stewartson, "On the Stability of a Spinning Top Containing Liquid," Journal of Fluid Mechanics, Vol. 5, Part 4, September 1959, pp. 577-592.*

2. *E. H. Wedemeyer, "Viscous Correction to Stewartson's Stability Criterion," Ballistic Research Laboratory, Aberdeen Proving Ground, Maryland, BRL Report No. 1325, June 1966. (AD 489687)*

3. *C. H. Murphy, "Angular Motion of a Spinning Projectile With a Viscous Liquid Payload," Ballistic Research Laboratory, Aberdeen Proving Ground, Maryland, BRL Memorandum Report ARBRL-MR-03194, August 1982. (AD A118676). (See also Journal of Guidance, Control, and Dynamics, Vol. 6, July-August 1983, pp. 280-286.)*

4. *C. W. Kitchens, Jr., N. Gerber, and R. Sedney, "Oscillations of a Liquid in a Rotating Cylinder: Solid Body Rotation," Ballistic Research Laboratory, Aberdeen Proving Ground, Maryland, BRL Technical Report BRL-TR-02081, June 1978. (AD A057759)*

5. *N. Gerber, R. Sedney, and J. M. Bartos, "Pressure Moment on a Liquid-Filled Projectile: Solid Body Rotation," Ballistic Research Laboratory, Aberdeen Proving Ground, Maryland, BRL Technical Report ARBRL-TR-02422, October 1982. (AD A120567)*

6. *N. Gerber and R. Sedney, "Moment on a Liquid-Filled Spinning and Nutating Projectile: Solid Body Rotation," Ballistic Research Laboratory, Aberdeen Proving Ground, Maryland, BRL Technical Report ARBRL-TR-02470, February 1983. (AD A125332)*

7. *C. H. Murphy, "Liquid Payload Roll Moment Induced by a Spinning and Coning Projectile," Ballistic Research Laboratory, Aberdeen Proving Ground, Maryland, BRL Technical Report ARBRL-TR-02521, September 1983. (AD A133681) (See also AIAA Paper 83-2142, August 1983.)*

8. *C. H. Murphy, "A Relationship Between Liquid Roll Moment and Liquid Side Moment," Ballistic Research Laboratory, Aberdeen Proving Ground, Maryland, BRL Memorandum Report ARBRL-MR-03347, April 1984. (AD A140658)*

An important limitation of this work has been the restriction to a single liquid in the payload. Scott[9] has derived relations for eigenfrequencies for two inviscid liquids and obtained fair experimental agreement. For Scott's inviscid liquids the tangential perturbation velocities have discontinuous jumps at the two-liquid interface.

In this report we will consider two viscous liquids, although we will restrict our consideration of viscosity to boundary layers near the cylindrical walls and near the two-liquid interface. The remainder of the liquid will be considered to be inviscid. Under these assumptions, side moment coefficients, as well as eigenfrequencies, will be computed.

II. LIQUID BOUNDARY CONDITIONS

Two coordinate systems will be used in this report: the nonrolling aeroballistic $\tilde{X}\tilde{Y}\tilde{Z}$ system whose $\tilde{X}$-axis is fixed along the missile's axis of symmetry and the inertial XYZ system whose X-axis is tangent to the trajectory at time zero. Both coordinate systems have origins at the center of the cylindrical payload cavity, which is assumed to be at the center of mass of the projectile. Location in the cavity can be specified in the aeroballistic system by the cylindrical coordinates $\tilde{x}$, $\tilde{r}$, $\tilde{\theta}$ and in the inertial system by x, r, θ. The boundary of the cavity is given by $\tilde{x} = \pm c$ and $\tilde{r} = a$ where 2c is the height of the cavity and 2a is its diameter. The projectile is assumed to be performing a coning motion of amplitude $K_1(t)$ and phase angle $\phi_1(t)$. If $\tilde{\alpha}$ and $\tilde{\beta}$ are the angles of attack and side-slip of the missile's axis with respect to the trajectory (the X-axis),

$$\tilde{\beta} + i\,\tilde{\alpha} = K_1 e^{i\phi_1} \tag{2.1}$$

$$= \hat{K}\, e^{s\phi}$$

where

$$\phi = \dot{\phi}t$$

$$s = (\varepsilon + i)\,\tau$$

$$\hat{K} = K_1(0)\, e^{i\phi_1(0)}$$

---

9. *W. E. Scott, "The Inertial Wave Frequency Spectrum in a Cylindrically Confined, Inviscid, Incompressible Two Component Liquid," Ballistic Research Laboratory, Aberdeen Proving Ground, Maryland, BRL Report No. 1609, September 1972. (AD 752439). (See also Physics of Fluids, Vol. 16, No. 1, pp. 9-12, January 1973.)*

$$\tau = \dot{\phi}_1 / \dot{\Phi}$$

$$\tau \varepsilon \dot{\Phi} = \dot{K}_1 / K_1 \ ,$$

and $\dot{\Phi}$ is the axial component of the angular velocity relative to inertia axes and is assumed to be positive and constant. Linear relations between cylindrical coordinates in the two coordinate systems were derived in Reference 3:

$$\tilde{x} = x - r\, K_1 \cos(\phi_1 - \vartheta) = x - r\, R\{\hat{K}\, e^{S\Phi}\} \tag{2.2}$$

$$\tilde{r} = r + x\, K_1 \cos(\phi_1 - \vartheta) = r + x\, R\{\hat{K}\, e^{S\Phi}\} \tag{2.3}$$

$$\tilde{\theta} = \vartheta + (x/r)\, K_1 \sin(\phi_1 - \vartheta) = \vartheta - (x/r)\, R\{i\hat{K}\, e^{S\Phi}\} \ , \tag{2.4}$$

where $R\{\ \} = [\{\ \} + \overline{\{\ \}}]/2$ is the real part of a complex quantity.

The two liquids have densities ρ_1 and $\rho_2 (\rho_1 \geq \rho_2)$ and kinematic viscosities ν_1 and ν_2. When the liquids are fully spun up and $K_1 = 0$, liquid 1 occupies the cylindrical annular region $b_1 \leq r \leq a$ and liquid 2 occupies a cylindrical annular region $b_2 \leq r \leq b_1$. The fill ratio, f, is the ratio of the volume of the annular region containing both liquids to that of the complete cylinder, i.e., $1 - (b_2/a)^2$. The surface $r = b_2$ is either a free surface or the surface of a rigid central rod. The free surface boundary will be considered in this report while the central rod will be discussed in Appendix A. For a fully filled cylinder, $b_2 = 0$ and $f = 1$.

When the cylinder is forced to perform a coning motion, the interface between the liquids is located at

$$r_1 = b_1 (1 + \eta_1) \tag{2.5}$$

where

$$|\eta_1 (x, \vartheta, t)| \ll 1 \ ,$$

and the free inner surface is located at

$$r_2 = b_2 (1 + \eta_2) \tag{2.6}$$

where

$$|\eta_2 (x, \vartheta, t)| \ll 1 .$$

The velocity components in the two liquids have a very simple form.

$$V_{xj} = R\ \{u_{js}\ e^{s\phi-i\theta}\}\ a\dot{\phi} \tag{2.7}$$

$$V_{rj} = R\ \{v_{js}\ e^{s\phi-i\theta}\}\ a\dot{\phi} \tag{2.8}$$

$$V_{\theta j} = \dot{\phi}\ r + R\ \{w_{js}\ e^{s\phi-i\theta}\}\ a\dot{\phi} \tag{2.9}$$

where $j = 1,2.$

The fluid pressure, however, has a more complicated form:

$$
\begin{aligned}
p &= p_0 && 0 \le r \le r_2 \\
&= p_0 + \rho_2\ \dot{\phi}^2 \left[\frac{r^2 - b_2^2}{2}\right] + R\ \{p_{2s} e^{s\phi-i\theta}\}\ \rho_2 a^2 \dot{\phi}^2 && r_2 \le r \le r_1 \\
&= p_0 + \rho_2\ \dot{\phi}^2 \left[\frac{b_1^2 - b_2^2}{2}\right] + \rho_2\ \dot{\phi}^2 \left[\frac{r^2 - b_1^2}{2}\right] \\
&\qquad + R\ \{p_{1s}\ e^{s\phi-i\theta}\}\ \rho_1\ a^2 \dot{\phi}^2 && r_1 \le r \le a\ .
\end{aligned}
\tag{2.10}
$$

If we assume the small perturbation of the interface surface has the same form as the perturbation velocities,

$$\eta_1 = R\ \{\eta_{1s}(x)\ e^{s\phi-i\theta}\}\ . \tag{2.11}$$

By use of Eqs. (2.3, 2.11), the equation of the interface surface is

$$
\begin{aligned}
F\ (x,r,\theta,t) &= r - b_1 - R\ \{b_1 \eta_{1s}\ e^{s\phi-i\theta}\} \\
&= 0.
\end{aligned}
\tag{2.12}
$$

At the interface, the two liquids have the same velocity, i.e., the velocity of the interface itself.

$$\therefore \frac{dF}{dt} = V_{xj}\,\frac{\partial F}{\partial x} + V_{rj}\,\frac{\partial F}{\partial r} + \frac{V_{\theta j}}{r}\,\frac{\partial F}{\partial \theta} + \frac{\partial F}{\partial t} = 0 \quad . \tag{2.13}$$

When only linear terms are retained, this reduces to

$$b_1\ \eta_{1s}(x) = \frac{a\ v_{1s}\ (b_1,\ x)}{s - i} = \frac{a\ v_{2s}\ (b_1,x)}{s - i} \quad . \tag{2.14}$$

Similarly, the perturbation of the inner surface has the form

$$b_2\ \eta_{2s}(x) = \frac{a\ v_{2s}\ (b_2,x)}{s - i} \tag{2.15}$$

where

$$\eta_2 = R\ \{\eta_{2s}\ e^{s\phi - i\theta}\} \quad .$$

In addition to three continuous velocity components at the interface, we will require the pressure and the two viscous shears to be continuous at the interface. Equations (2.10, 2.14) yield a simple pressure relation at the interface:

$$p_{1s}\ (b_1,x) + \frac{b_1\ v_{1s}(b_1,x)}{a(s - i)} = \rho_{21}\left[p_{2s}(b_1,x) + \frac{b_1\ v_{2s}(b_1,x)}{a\ (s - i)}\right] \tag{2.16}$$

where $\rho_{21} = \rho_2/\rho_1$.

If only velocity gradients normal to the interface are considered, the continuous viscous shear assumptions imply that

$$\mu_1\ \frac{\partial\ u_{1s}(b_1,x)}{\partial\ r} = \mu_2\ \frac{\partial\ u_{2s}(b_1,x)}{\partial\ r} \tag{2.17}$$

$$\mu_1\ \frac{\partial\ w_{1s}(b_1,x)}{\partial\ r} = \mu_2\ \frac{\partial\ w_{2s}(b_1,x)}{\partial\ r} \quad . \tag{2.18}$$

At the free surface, the pressure is constant and the viscous shears are zero.

$$p_{2s}(b_2,x) + \frac{b_2 v_{2s}(b_2,x)}{a\ (s - i)} = 0 \tag{2.19}$$

$$\mu_2 \frac{\partial\ u_{2s}(b_2,x)}{\partial\ r} = 0 \tag{2.20}$$

$$\mu_2 \frac{\partial\ w_{2s}(b_2,x)}{\partial\ r} = 0. \tag{2.21}$$

Finally, at the cylinder surface the liquid must have the rigid body motion of the cylinder.

$$u_{1s} = (s - i)\ \hat{K} \tag{2.22}$$

$$v_{1s} = -(s - i)\ (x/a)\ \hat{K} \tag{2.23}$$

$$w_{1s} = i(s - i)\ (x/a)\ \hat{K}. \tag{2.24}$$

III. THE INVISCID SOLUTION

The perturbation functions are written as sums of viscous and inviscid parts.

$$\begin{aligned} u_{js} &= u_{jsi} + u_{jsv} & \qquad w_{js} &= w_{jsi} + w_{jsv} \\ v_{js} &= v_{jsi} + v_{jsv} & \qquad p_{js} &= p_{jsi} + p_{jsv}. \end{aligned} \tag{3.1}$$

The differential equations for the inviscid functions of each liquid are the same as those for a single liquid and the solutions have the same form.[3]

More specifically, the pressure and velocity perturbations are expressed as the sum of products of functions of x and functions of r. The functions of x are 1, x/a, sin $(\lambda_{jk}\ x/a)$, and cos $(\lambda_{jk}\ x/a)$ where

$$\lambda_{jk} = (\pi k/2)\ [1 + \delta_{cj}]\ ; \qquad k = 1,3,5...(2N_k-1) \tag{3.2}$$

$$\delta_{cj} = \frac{-(a/c)\ (1+i)}{2\sqrt{2}\ (1 + is)} \left\{ \frac{1 - is}{\sqrt{3 + is}} + \frac{i(3 + is)}{\sqrt{1 - is}} \right\} Re_j^{-1/2} \tag{3.3}$$

$$Re_j = \frac{a^2 \dot{\phi}}{\nu_j}. \tag{3.4}$$

The specific expressions for pressure and velocity functions are given in Table 1.

TABLE 1. INVISCID PERTURBATION FUNCTIONS*

$$p_{jsi} = -\left[(i-s)^2 (x/c)(r/a) + \Sigma R_{jk}(r) \sin(\lambda_{jk} x/c)\right] (c/a) \hat{K}$$

$$u_{jsi} = -\left[(i-s)(r/a) + (i-s)^{-1} \Sigma R_{jk} \lambda_k \cos(\lambda_{jk} x/c)\right] \hat{K}$$

$$v_{jsi} = \left[(i-s)^2 (i+s)^{-1} (x/c) + \Sigma R_{vjk} \sin(\lambda_{jk} x/c)\right] (c/a) \hat{K}$$

$$w_{jsi} = \left[-i (i-s)^2 (i+s)^{-1} (x/c) + \Sigma R_{wjk} \sin(\lambda_{jk} x/c)\right] (c/a) \hat{K}$$

$$R_{jk} = E_{jk} J_1(\hat{r}) + F_{jk} Y_1(\hat{r})$$

$$R_{vjk} = \left[(s-i)\, a R'_{jk} - 2i(a/r) R_{jk}\right] S^{-1}$$

$$R_{wjk} = -\left[2a R'_{jk} + i(s-i)(a/r) R_{jk}\right] S^{-1}$$

$$\hat{r} = \hat{\lambda}_{jk} r/c$$

$$\hat{\lambda}_{jk}{}^2 = -\left[\frac{S}{(s-i)^2}\right] \lambda_{jk}{}^2$$

$$S = s^2 - 2is + 3.$$

If $\nu_1 \neq \nu_2$, the λ_{jk}'s for the same k are not the same, the trigonometric functions on opposite sides of the liquid interface are slightly different, and the interface boundary conditions require a special least squares process. In the body of this report, we will use a single λ_k determined by an average kinematic viscosity, ν_a.

$$\lambda_k = (\pi k/2)\left[1 + \delta_{c1} (\nu_a/\nu_1)^{1/2}\right] \tag{3.5}$$

---

*The conditions for the E_{jk}'s and F_{jk}'s are given in Section [illegible]. Note that the definitions of E_{jk} and F_{jk} in [illegible] differ from those of E_k and F_k of Reference [illegible].

where

$$\nu_a = \frac{\nu_1 (a^2 - b_1^2) + \nu_2 (b_1^2 - b_2^2)}{a^2 - b_2^2} .$$

In Appendix B, a much more accurate treatment of unequal viscosities will be described.

IV. THE VISCOUS SOLUTION

In Reference 3 the viscous parts of the perturbation variables were important only in a small region near the cylinder wall and the endwalls, and these functions were computed by the use of unsteady boundary layer equations in these regions. It is reasonable to expect that the viscous parts can also have contributions near the liquid interface and that derivatives in the radial direction are much larger than those in the circumferential or axial directions. Thus, we will assume that the viscous functions away from the endwalls satisfy the same equations as those for the cylindrical wall boundary layers.[3]

$$(s - i)\, w_{jsv} = a^2\, Re_j^{-1}\, \frac{\partial^2 w_{jsv}}{\partial r^2} \tag{4.1}$$

$$(s - i)\, u_{jsv} = a^2\, Re_j^{-1}\, \frac{\partial^2 u_{jsv}}{\partial r^2} \tag{4.2}$$

$$a\, \frac{\partial p_{jsv}}{\partial r} = 2\, w_{jsv} . \tag{4.3}$$

The solutions to Eqs. (4.1 - 4.3) are

$$w_{1sv} = w_{10}\, e^{\frac{r - a}{a\, \delta_{a1}}} + w_{11}\, e^{\frac{-(r - b_1)}{a\, \delta_{a1}}} \tag{4.4}$$

$$w_{2sv} = w_{21}\, e^{\frac{r - b_1}{a\, \delta_{a2}}} + w_{22}\, e^{\frac{-(r - b_2)}{a\, \delta_{a2}}} \tag{4.5}$$

$$u_{1sv} = u_{10}\, e^{\frac{r - a}{a\, \delta_{a1}}} + u_{11}\, e^{\frac{-(r - b_1)}{a\, \delta_{a1}}} \tag{4.6}$$

$$u_{2sv} = u_{21}\, e^{\frac{r - b_1}{a\,\delta_{a2}}} + u_{22}\, e^{\frac{-(r - b_2)}{a\,\delta_{a2}}} \tag{4.7}$$

$$p_{1sv} = 2\,\delta_{a1}\left[w_{10}\, e^{\frac{r - a}{a\,\delta_{a1}}} - w_{11} e^{\frac{-(r - b_1)}{a\,\delta_{a1}}}\right] \tag{4.8}$$

$$p_{2sv} = 2\,\delta_{a2}\left[w_{21} e^{\frac{r - b_1}{a\,\delta_{a2}}} - w_{22} e^{\frac{-(r - b_2)}{a\,\delta_{a2}}}\right], \tag{4.9}$$

where $\delta_{aj} = \left[\frac{1 + i}{\sqrt{2}\,(1 + is)}\right] Re_j^{\ -1/2}$,

and the eight coefficients u_{jk}, w_{jk} are functions of x. Four conditions on the coefficients come from the continuity of tangential velocities and shears [Eqs. (2.17 - 2.18)] at the interface.

$$\Delta w_{si} + w_{10}\,\varepsilon_1 + w_{11} - w_{21} - w_{22}\,\varepsilon_2 = 0 \tag{4.10}$$

$$\Delta u_{si} + u_{10}\,\varepsilon_1 + u_{11} - u_{21} - u_{22}\,\varepsilon_2 = 0 \tag{4.11}$$

$$w_{10}\,\varepsilon_1 - w_{11} = N\,(w_{21} - w_{22}\,\varepsilon_2) \tag{4.12}$$

$$u_{10}\,\varepsilon_1 - u_{11} = N\,(u_{21} - u_{22}\,\varepsilon_2) \tag{4.13}$$

where

$$\Delta w_{si} = [w_{1si} - w_{2si}]_{r = b_1}$$

$$\Delta u_{si} = [u_{1si} - u_{2si}]_{r = b_1}$$

$$\epsilon_1 = e^{\frac{b_1 - a}{a\ \delta_{a1}}}$$

$$\epsilon_2 = e^{\frac{b_2 - b_1}{a\ \delta_{a2}}}$$

$$N = \rho_{21} \sqrt{\nu_2/\nu_1} \ .$$

Four more conditions come from the no-slip condition at the cylindrical wall [Eqs. (2.22, 2.24)] and the no-shear condition of the free surface [Eqs. (2.20 - 2.21)] .

$$w_{1si}(a,x) + w_{10} + w_{11}\ \epsilon_1 = i(s - i)\hat{K}(x/a) \ . \tag{4.14}$$

$$u_{1si}(a,x) + u_{10} + u_{11}\ \epsilon_1 = (s - i)\ \hat{K}. \tag{4.15}$$

$$w_{21}\ \epsilon_2 - w_{22} = 0 \ . \tag{4.16}$$

$$u_{21}\ \epsilon_2 - u_{22} = 0. \tag{4.17}$$

Eqs. (4.10 - 4.17) can now be used to determine the eight coefficient functions. If the total liquid occupies an annular region that is thicker than ten boundary layer thicknesses, the product $\epsilon_1\ \epsilon_2$ is quite small and can be neglected. The resulting expressions for the coefficient functions are given in Table 2. If the liquid interface is more than ten boundary layer thicknesses from both the cylindrical surface and the free surface, both ϵ_1 and ϵ_2 are very small and can be neglected in Table 2.

Eqs. (4.8 - 4.9) can be used in conjunction with Eqs. (4.12,4.16) to yield general relations for the viscous perturbation pressures at the three boundaries.

$$p_{2sv}\ (b_2,x) = 0 \ . \tag{4.18}$$

$$p_{1sv}\ (b_1,x) = \rho_{21}\ p_{2sv}\ (b_1,x) \ . \tag{4.19}$$

$$p_{1sv}\ (a,x) = 2\ \delta_{a1}\ (w_{10} - w_{11}\ \epsilon_1) \ . \tag{4.20}$$

TABLE 2. VISCOUS COEFFICIENT FUNCTIONS FOR INTERNAL FREE SURFACE.

$$w_{10} = \{[1 + N + (1 - N)\,\varepsilon_2^{\,2}]w_a + N\,\varepsilon_1\,\Delta\,w_{si}\}D^{-1}$$

$$w_{11} = \{(1 - N)\,\varepsilon_1\,w_a - N\,(1 - \varepsilon_2^{\,2})\,\Delta\,w_{si}\}\,D^{-1}$$

$$w_{21} = \{2\,\varepsilon_1\,w_a + (1 + \varepsilon_1^{\,2})\,\Delta\,w_{si}\}\,D^{-1}$$

$$w_{22} = \varepsilon_2\,\Delta\,w_{si}\,D^{-1}$$

$$u_{10} = \{[1 + N + (1 - N)\,\varepsilon_2^{\,2}]\,u_a + N\,\varepsilon_1\,\Delta\,u_{si}\}\,D^{-1}$$

$$u_{11} = \{(1 - N)\,\varepsilon_1 u_a - N\,(1 - \varepsilon_2^{\,2})\,\Delta\,u_{si}\}D^{-1}$$

$$u_{21} = \{2\,\varepsilon_1\,u_a + (1 + \varepsilon_1^{\,2})\,\Delta\,u_{si}\}\,D^{-1}$$

$$u_{22} = \varepsilon_2\,\Delta\,u_{si}\,D^{-1}$$

$$v_{10} = \{[1 + N + (1 - N)\,\varepsilon_2^{\,2}]\,v_a + N\,\varepsilon_1\Delta^*\}\,D^{-1}$$

$$v_{11} = \{-(1 - N)\,\varepsilon_1\,v_a + N\,(1 - \varepsilon_2^{\,2})\,\Delta^*\}\,D^{-1}$$

$$v_{21} = \{2\,\varepsilon_1 v_a + (1 + \varepsilon_1^{\,2})\,\Delta^*\}\,D^{-1}$$

$$v_{22} = -\varepsilon_2\,\Delta^*\,D^{-1}$$

---

where

$$w_a = i\,(s - i)\,(x/a)\,\hat{K} - w_{1si}\,(a,x)$$

$$u_a = (s - i)\,\hat{K} - u_{1si}\,(a,x)$$

$$v_a = -(s - i)\,(x/a)\,\hat{K} - \left[\frac{\partial\,(r\,v_{1si})}{\partial r}\right]_{r\,=\,a}$$

$$D = 1 + N + (1 - N)\,(\varepsilon_1^{\,2} + \varepsilon_2^{\,2})$$

$$\Delta^* = \left[\frac{\partial\,(r\,v_{1si})}{\partial\,r} - \frac{\partial\,(r\,v_{2si})}{\partial\,r}\right]_{r\,=\,b_1}$$

In order to compute the viscous radial velocity, we must use an inequality involving the magnitude of a complex exponential. From the definition of δ_{aj}

$$\left|\exp\left\{-\frac{\Delta r}{a\ \delta_{aj}}\right\}\right| = \exp\left\{\frac{-2^{-1/2}\Delta r}{a\,|\delta_{aj}|}\right\} \tag{4.21}$$

$$\therefore\ \left|\frac{\Delta r}{a}\exp\left\{-\frac{\Delta r}{a\ \delta_{aj}}\right\}\right| = 2^{1/2}\ |\delta_{aj}|\ z\ e^{-z} < |\delta_{aj}| \tag{4.22}$$

where $z = 2^{-1/2}\,\frac{\Delta r}{a}\,|\delta_{aj}|^{-1} > 0$.

Equations (4.4 - 4.7) can now be substituted in the continuity equation. The results can then be integrated and simplified by use of Inequality (4.22) and neglecting $|\delta_{aj}|^2$ terms.

$$r\ v_{1sv} = a\delta_{a1}\left[v_{10}\ e^{\frac{r-a}{a\ \delta_{a1}}} + v_{11}e^{\frac{-(r-b_1)}{a\ \delta_{a1}}}\right] \tag{4.23}$$

$$r\ v_{2sv} = a\delta_{a2}\left[v_{21}e^{\frac{r-b_1}{a\ \delta_{a2}}} + v_{22}\ e^{\frac{-(r-b_2)}{a\ \delta_{a2}}}\right] \tag{4.24}$$

where $v_{10} = \ i\ w_{10} - a\ u'_{10}$

$v_{11} = -[i\ w_{11} - b_1\ u'_{11}]$

$v_{21} = \ i\ w_{21} - b_1\ u'_{21}$

$v_{22} = -[i\ w_{22} - b_2\ u'_{22}]$.

Eqs. (4.23 - 4.24) can now be used in conjunction with Eqs. (4.11, 4.13 - 4.17) to give relations for the radial viscous velocity at the three boundaries.

$$v_{2sv}\ (b_2,x) = 0 \tag{4.25}$$

$$\begin{aligned} v_{1sv}\ (b_1,x) &= \rho_{21}\ v_{2sv}\ (b_1,x) \\ &= \rho_{21}\ [v_{21} + \varepsilon_2\ v_{22}]\ (a/b_1)\ \delta_{a2} \end{aligned} \tag{4.26}$$

$$v_{1sv}\ (a,x) = [v_{10} + v_{11}\ \varepsilon_1]\ \delta_{a1} \tag{4.27}$$

where v_{jk} are given in Table 2 (relation (4.22) was used to simplify entries in this table).

V. INVISCID BOUNDARY CONDITIONS

In the previous section, we used eight of the twelve liquid boundary conditions to determine the viscous perturbations in terms of the inviscid perturbations. We will now completely determine the inviscid perturbation by use of the remaining four conditions--Eqs. (2.16, 2.19, 2.23) and $v_{1s} = v_{2s}$ at the interface. These conditions can be simply stated by use of Eqs. (4.18, 4.19, 4.25, 4.26):

at $r = b_1$

$$p_{1si} + \frac{b_1\ v_{1si}}{a\ (s - i)} = \rho_{21}\left[p_{2si} + \frac{b_1\ v_{2si}}{a\ (s - i)}\right] \tag{5.1}$$

$$v_{1si} = v_{2si} + (1 - \rho_{21})\ v_{2sv} \tag{5.2}$$

at $r = b_2$

$$p_{2si} + \frac{b_2\ v_{2si}}{a\ (s - i)} = 0 \tag{5.3}$$

at $r = a$

$$v_{1si} + v_{1sv} = (i - s)\ (x/a)\ \hat{K}\ . \tag{5.4}$$

Eqs. (5.1 - 5.4) with v_{1sv} and v_{2sv} set equal to zero were used by Scott[9] to obtain eigenfrequencies for a completely inviscid liquid payload. As can be seen from Table 1, for each k four constants must be determined to completely determine the inviscid perturbation functions, i.e., E_{1k}, E_{2k}, F_{1k}, F_{2k}. (For the special case of 100% filled cylinder ($b_2 = 0$), F_{2k} is zero and

instead of $4N_k$ constants only $3N_k$ constants remain to be determined.) To obtain these conditions, we fit (x/c) to a series in $\sin(\lambda_k x/c)$ by least squares

$$x/c = \Sigma\, a_k \sin(\lambda_k x/c) \; . \tag{5.5}$$

Next, Eq. (5.5) and the corresponding expansions for the pressure and velocity functions from Table 1 are substituted in Eqs. (5.1-5.4) and coefficients are equated.

$$R_{1k}(b_1) - \rho_{21} R_{2k}(b_1) - (b_1/a)[R_{v1k}(b_1) - \rho_{21} R_{v2k}(b_1)](s-i)^{-1} = \frac{(1-\rho_{21})\, s^2 (i-s)}{i+s} (b_1/a)\, a_k \tag{5.6}$$

$$R_{v1k}(b_1) - R_{v2k}(b_1) - (1-\rho_{21})\, \delta_{a2} R_k^{*} = (1-\rho_{21})\, \varepsilon_1\, \delta_{a2} A_1 a_k \tag{5.7}$$

$$R_{2k}(b_2) - (b_2/a)\,(s-i)^{-1} R_{v2k}(b_2) = \frac{s^2 (i-s)}{i+s} (b_2/a)\, a_k \tag{5.8}$$

$$R_{v1k}(a) - A_2\, \delta_{a1} a\, R'_{v1k}(a) + \varepsilon_1 N\, \delta_{a1} R_k^{**} D_0^{-1} = \frac{2s\,(i-s)}{i+s}\, a_k \, , \tag{5.9}$$

where

$$R_k^{*} = \{(1+\varepsilon_1^{\,2} - \varepsilon_2^{\,2})\, a\, [R'_{v1k}(b_1) - R'_{v2k}(b_1)]$$

$$- 2\, \varepsilon_1 (a/b_1)[R_{v1k}(a) + a\, R'_{v1k}(a)]\}\, D_1^{-1}$$

$$R_k^{**} = 2\,[R_{v1k}(b_1) + b_1 R'_{v1k}(b_1) - R_{v2k}(b_1) - b_1 R'_{v2k}(b_1)]$$

$$A_1 = 4\,(a/b_1) \left[\frac{s\,(i-s)}{i+s}\right] D_1^{-1}$$

$$A_2 = [1 + N + (1 - N)\ (\epsilon_2^2 - \epsilon_1^2)]\ D_0^{-1}$$

$$D_0 = D - \delta_{a1}\ [1 + N - (1 - N)(\epsilon_1^2 - \epsilon_2^2)]$$

$$D_1 = D - (1 - \rho_{21})(1 + \epsilon_1^2 - \epsilon_2^2).$$

VI. LIQUID MOMENT

For coning motion described by Eq. (2.1), the linear liquid pitch and yaw moment is defined to be:[3]

$$M_{L\tilde{Y}} + i\ M_{L\tilde{Z}} = m_L a^2 \dot{\phi}^2 \tau\ (C_{LSM} + iC_{LIM})\hat{K}\ e^{is\phi} \tag{6.1}$$

where $m_L = 2\pi\ \rho_1 a^2 c$.

The major components of this liquid moment are due to the pressure on the lateral wall and the endwalls of the container. Lesser components are due to the viscous wall shear on the lateral and endwalls. Thus, the liquid moment coefficient can be given as a sum of four terms. (For simplicity these terms will be computed for the center of the cylinder at the center of mass of the projectile. More complete expressions are given in Reference 3.)

$$\tau\ (C_{LSM} + i\ C_{LIM}) = m_{p\ell} + m_{pe} + m_{v\ell} + m_{ve}\,. \tag{6.2}$$

By use of Eqs. (2.2 - 2.4) and Eq. (2.10), the linear periodic part of the pressure can be computed in cylinder-fixed coordinates

$$\frac{\Delta p_i}{\rho_1 a^2 \dot{\phi}^2} = R\ \{[\tilde{p}_{1si}\ (\tilde{r},\tilde{x})]\ e^{s\phi - i\tilde{\theta}}\} \qquad \text{for } b_1 < \tilde{r} < a$$

$$= \rho_{21}\ R\ \{[\tilde{p}_{2si}\ (\tilde{r},\tilde{x})]\ e^{s\phi - i\tilde{\theta}}\} \qquad \text{for } b_2 < \tilde{r} < b_1 \tag{6.3}$$

where $\tilde{p}_{jsi}\ (\tilde{r},\tilde{x}) = p_{jsi}\ (\tilde{r},\tilde{x}) - (\tilde{r}\tilde{x}/a^2)\ \hat{K}$.

Eq. (6.3) for the inviscid pressure and Eq. (4.8) for the viscous lateral wall pressure can be integrated to yield the pressure moment coefficient on the lateral wall.

$$m_{p\ell} = i\ (2\ ac\hat{K})^{-1} \int_{-c}^{c} \tilde{x}\ [\tilde{p}_{1si}\ (a,\tilde{x}) + p_{1sv}\ (a,\tilde{x})]\ d\tilde{x} \tag{6.4}$$

where $p_{1sv}\ (a,\tilde{x}) = 2\ \delta_{a1}\ (w_{10} - w_{11}\varepsilon_1)$.

Since the viscous pressure on the endwalls is zero, the expression for the pressure moment coefficient on the endwalls is slightly simpler.

$$m_{pe} = -\ i\ (a^2c\hat{K})^{-1} \left\{ \int_{b_1}^{a} \tilde{p}_{1si}\ (\tilde{r},c)\ \tilde{r}^2\ d\tilde{r} + \rho_{21} \int_{b_2}^{b_1} \tilde{p}_{2si}\ (\tilde{r},c)\ \tilde{r}^2\ d\tilde{r} \right\}. \tag{6.5}$$

The viscous moment coefficient on the lateral wall can be computed by use of Eqs. (4.4) and (4.6).

$$m_{v\ell} = (2ac\hat{K}\ Re_1\ \delta_{a1})^{-1} \int_{-c}^{c} [ia\ (u_{10} - \varepsilon_1\ u_{11}) + \tilde{x}\ (w_{10} - \varepsilon_1\ w_{11})]\ d\tilde{x}. \tag{6.6}$$

The viscous moment coefficient on the endwalls is a little more difficult to compute since a change in kinematic viscosity can occur across the interface as well as a change in density. The relations of Reference 3 can, however, be used to obtain the following result.

$$m_{ve} = \left(\frac{\sqrt{i + s}}{a^2\ \hat{K}}\right) Re_1^{-1/2} \left[\int_{b_1}^{a} w_1\ (\tilde{r})\ \tilde{r}\ d\tilde{r} + N \int_{b_2}^{b_1} w_2\ (\tilde{r})\ \tilde{r}\ d\tilde{r} \right] \tag{6.7}$$

where

$$w_j(\tilde{r}) = 2(1+is)(c/a)\ \hat{K} - w_{jsi}(\tilde{r},c) + i\ v_{jsi}(\tilde{r},c).$$

VII. DISCUSSION

[illegible] s, Eqs. (5.6 - 5.9) yield values of E_{1k}, E_{2k}, [illegible] component of the liquid moment. Values of s that make the four by four determinant of the system zero are called [illegible], where k is the axial mode number and n is the radial mode number. [illegible] parts of the s_{kn}'s are frequencies, τ_{kn}, of the transient motion in the liquid and the real parts are the damping rates of that motion. (For a single liquid, τ_{k1} is the smallest τ_{kn} and τ_{kn} increases monotonically with increasing n.) When the forced coning motion of the projectile has a frequency near an eigenfrequency, the liquid side moment has a local maximum. For this reason, the eigenfrequencies are of considerable interest to a projectile designer.*

The equations of this paper have been coded for the VAX 11/780 computer and eigenfrequencies can be computed for specified values of c/a, Re, k, ρ_{21}, N, b_1/a, and b_2/a. Codes for both an interior free surface and rigid rod are available. In Figs. 1 - 3, sample plots of τ_{31} are given for a fineness ratio of 3.1 and Reynolds number of 40,000. Each figure plots τ_{31} versus the location of the liquid interface for three values of ρ_{21}.

In Figure 1, we see that for a fully-filled container, τ_{31} has the single-liquid value of .035 at $b_1/a = 0,1$ and reaches a maximum value for $b_1/a = .75$. Thus, the maximum change in eigenfrequency occurs when there are approximately equal volumes of the two liquids.

A fill ratio of 98% ($b_2/a = .141$) is considered for a free surface (Fig. 2) and a central rod (Fig. 3). Although there is very little change from the fully-filled case for the free surface, the central rod has a strong effect. For all density ratios, the single-liquid eigenfrequency of .113 occurs for three values of b_1/a (0, .53, 1) and the maximum effect is at .8.

---

* [illegible] frequencies have the azimuthal [illegible], proportional to $e^{im\theta}$ (m = 1). [illegible] theoretical interest. [illegible] in Appendix C and [illegible]

Scott's experimental data were for $c/a = 3.127$, $Re_i = 2 \cdot 10^6$, $\rho_{21} = .82$, and $f = 0.9$, 1. (The second, third, and fourth columns of Scott's Table I are mis-labeled in Reference 9. In his notation, they should be identified as d/c, bdc^{-2}, and adc^{-2}.) His data are compared with the theory of this paper in Figure 4, and we see that the maximum error is 1% . In Reference 3 it was found that much better fits could be obtained by using a slightly different value of the fineness ratio. Indeed, effective values of fineness ratio which were 0.5% greater than the measured value would give excellent agreement. In Figure 4 it is shown that a 0.7% greater fineness ratio ($c/a = 3.150$) gives excellent agreement for six different experiments.

An important characteristic of an eigenfrequency is the occurrence of a maximum side moment coefficient for a coning motion with constant damping and a frequency near the eigenfrequency. The theory of this report was used to compute the maximum side moment coefficients for the conditions of Figure 1 and constant amplitude coning motion with frequency near τ_{31}. The resulting curves are given in Figure 5 and have a number of interesting properties.

As b_1/a varies from 0 to 1, the heavier liquid is replaced by the lighter liquid. Since the side moment is defined in terms of the density ρ_1 of the heavier liquid, a requirement for our C_{LSM} (b_1/a) is that

$$C_{LSM}(1) = \rho_{21} \, C_{LSM}(0) \, . \tag{7.1}$$

This requirement was satisfied by our calculations. It is important to note that a large change in side moment occurs when the liquid interface is near the cylindrical wall and the interface boundary layer overlaps the wall boundary layer. Therefore, small amounts of heavier liquid can have a large effect on the side moment exerted by a spinning liquid payload.

An interesting feature of the $\rho_{21} = .4$ side moment coefficient curve is the presence of two small peaks. These are caused by the equality of τ_{31} and τ_{52} for these locations of the interface. Figure 6 compares the complete dependence of τ_{52} on interface location with that of τ_{31} for $\rho_{21} = .4$. For $n = 1$ the eigenfrequency has one maximum, while for $n = 2$ the corresponding eigenfrequency has two maxima, and for small enough density ratio those eigenfrequency curves can intersect.

The coalescence of eigenfrequencies for special interface locations also occurs for the fineness ratio of 4.29, which has been extensively studied by

[illegible] the primary eigenfrequency of inter- [illegible] Figure 7 for three density ratios. This [illegible] as the single-liquid [illegible] density ratios. Eigenfrequency τ_{72} is [illegible] for τ_{21} = [illegible] in Figure 8. This n = 3 [illegible] intersections with τ_{72}. On Figure 9, [illegible] is plotted versus b_1/a for three [illegible] the presence of an eigenfrequency [illegible]

Measurements of gyroscope damping rate produced by a mixture of oil and water [illegible] made by Kayser [illegible].[14] For a mixture of 15% silicon oil [illegible] damping rate is plotted versus τ in Figure 10. This mixture [illegible] container mounted in the gyroscope. The theoretical side moment can be used to predict the damping rate, and this prediction is shown as the dashed curve. The shape of the curve is good but there is a frequency bias of .0025. This bias corresponds to changing the fineness ratio 0.3% from the actual value of 3.126 to an effective value of 3.135.

VIII. SUMMARY

1. A linear boundary layer theory has been developed for a two-liquid payload that is coning and spinning.

2. The predicted eigenfrequencies and side moments agree well with available experiments except for an unexplained frequency bias.

3. Large changes in side moments can be caused by the presence of a small amount of heavier liquid.

4. For certain locations of the liquid interface, pairs of eigenfrequencies can coalesce.

[illegible]

ACKNOWLEDGMENT

The author is deeply indebted to Mr. James W. Bradley for checking most of the equations of this paper and coding all the calculations on the VAX 11/780 computer. The correct equations and calculations are the result of Mr. Bradley's very capable efforts while any errors are blunders on the author's part.

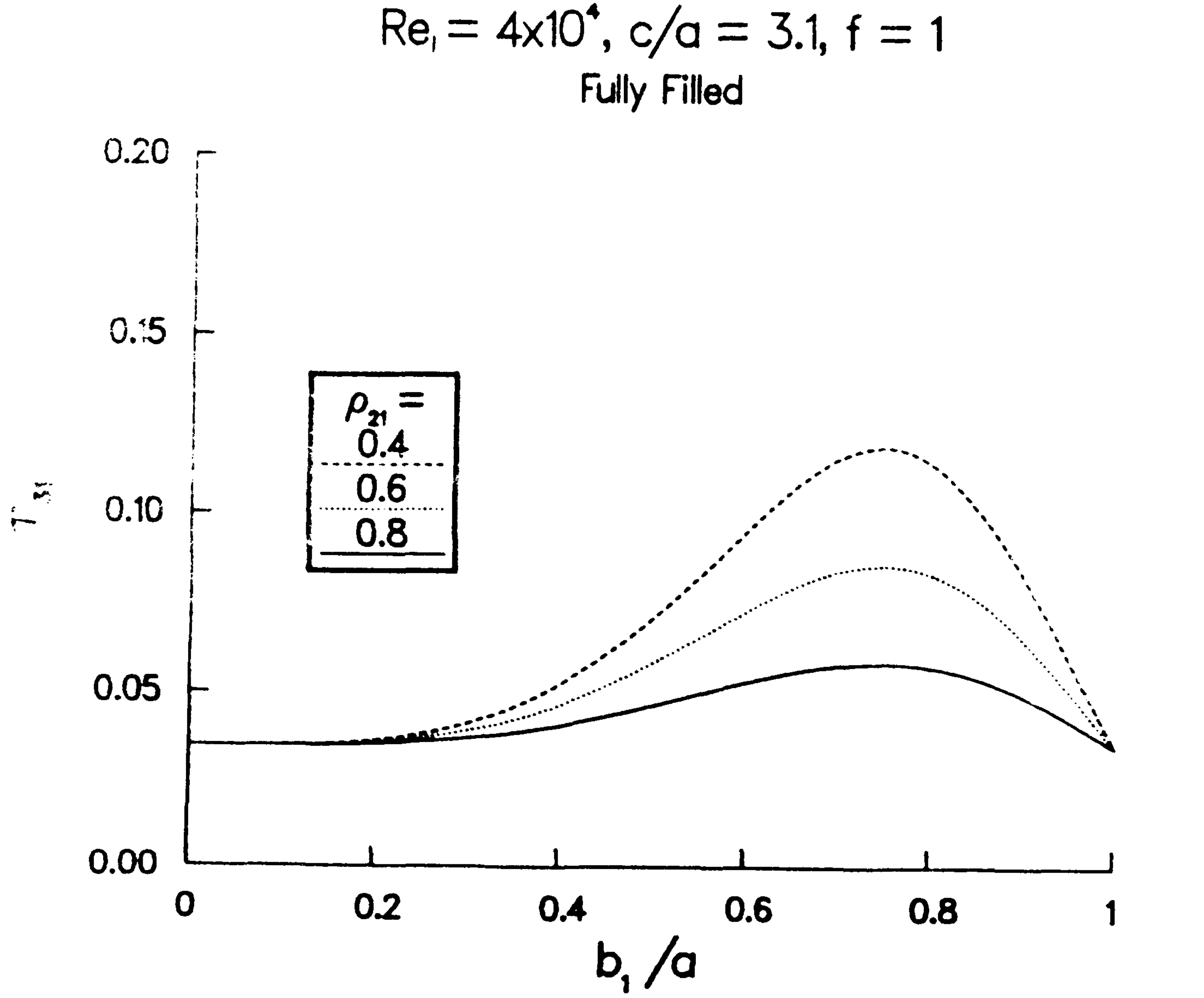

Figure 1. τ_{31} versus b_1/a for $Re_1 = 4 \times 10^4$, $c/a = 3.1$, $f = 1$ and Various Density Ratios.

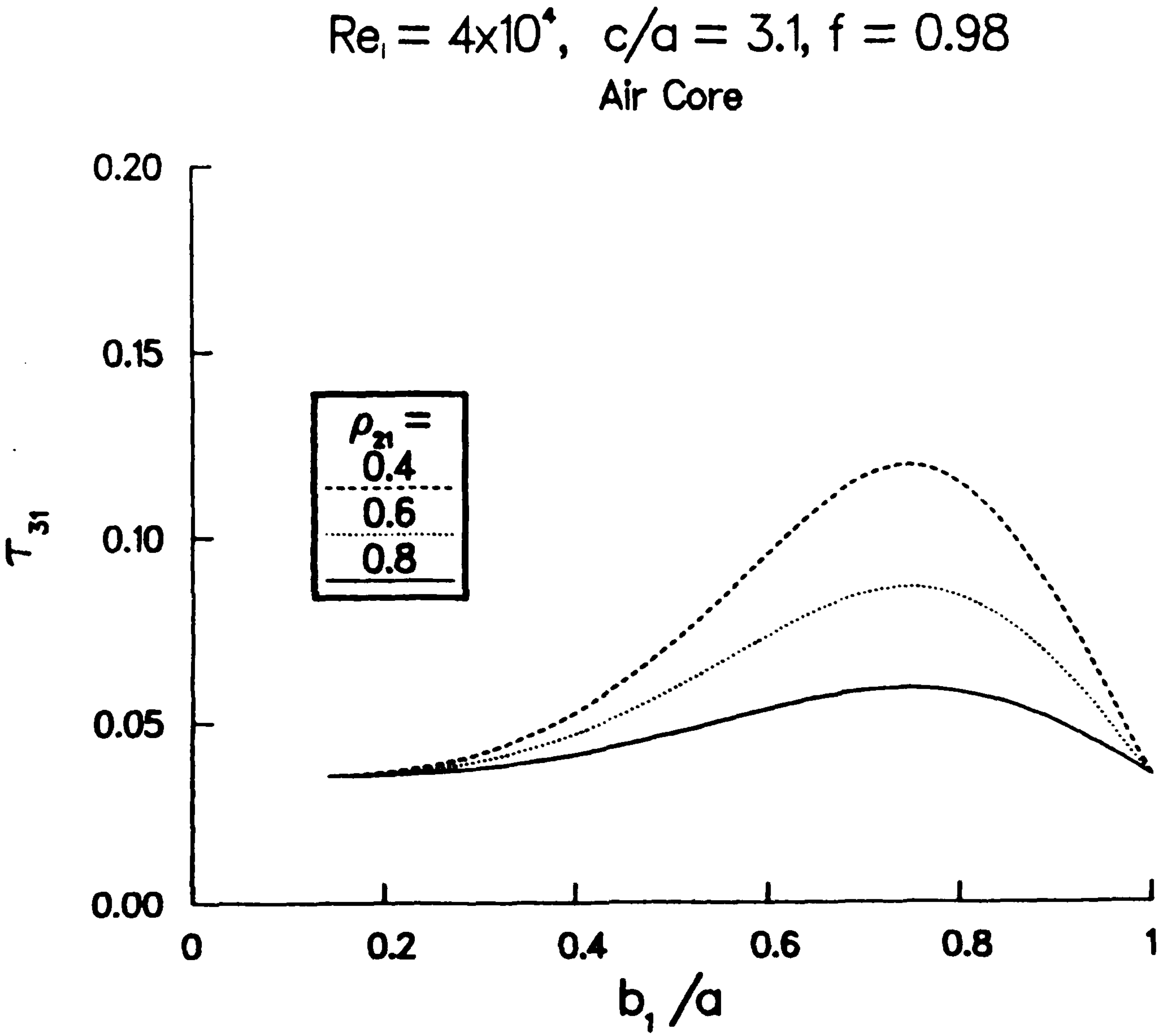

Figure 2. τ_{31} versus b_1/a for $Re_1 = 4 \times 10^4$, $c/a = 3.1$, $f = .98$ with a Free Surface and Various Density Ratios.

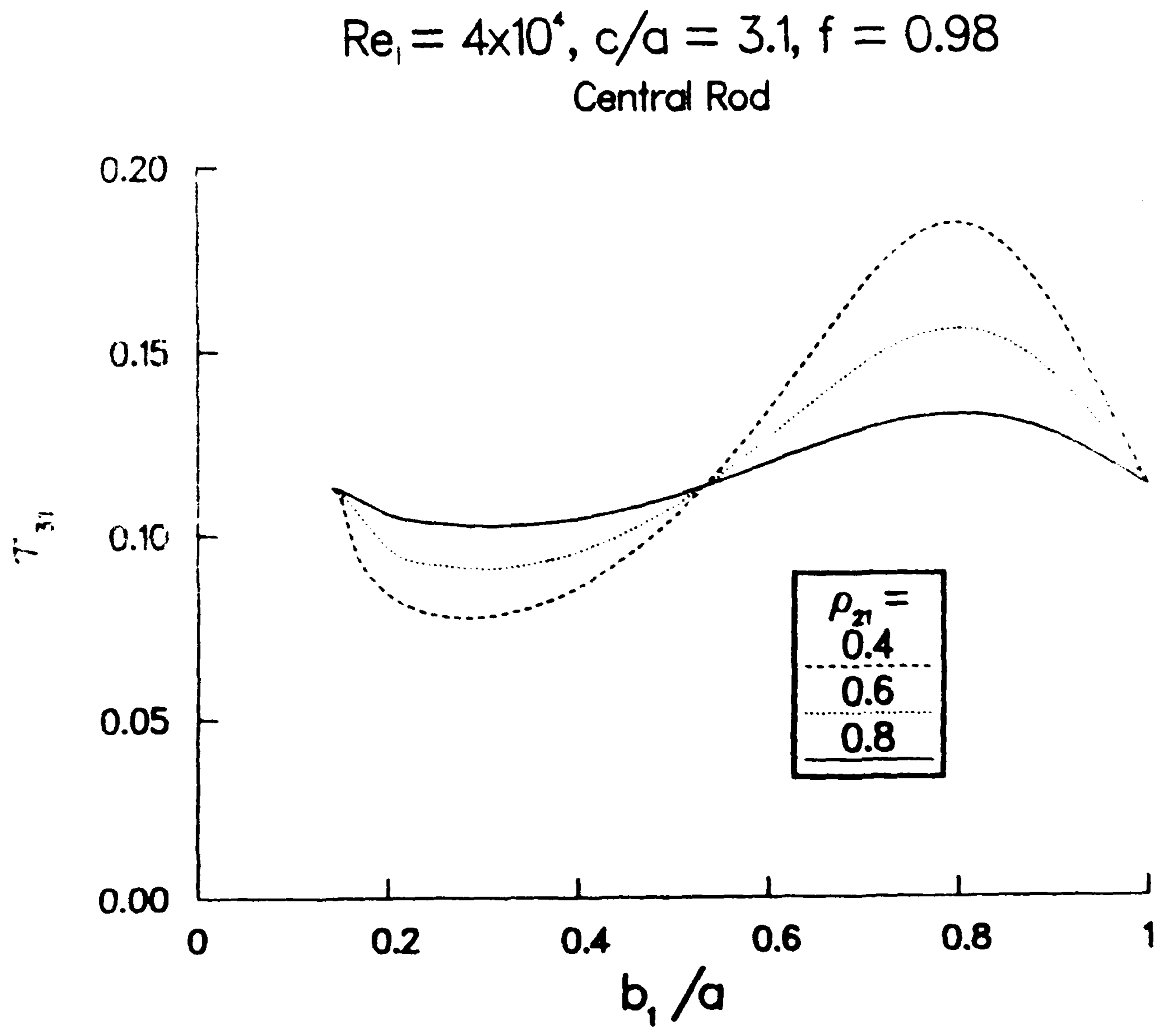

Figure 3. τ_{31} versus b_1/a for $Re_1 = 4 \times 10^4$, $c/a = 3.1$, $f = .98$ with a Central Rod and Various Density Ratios.

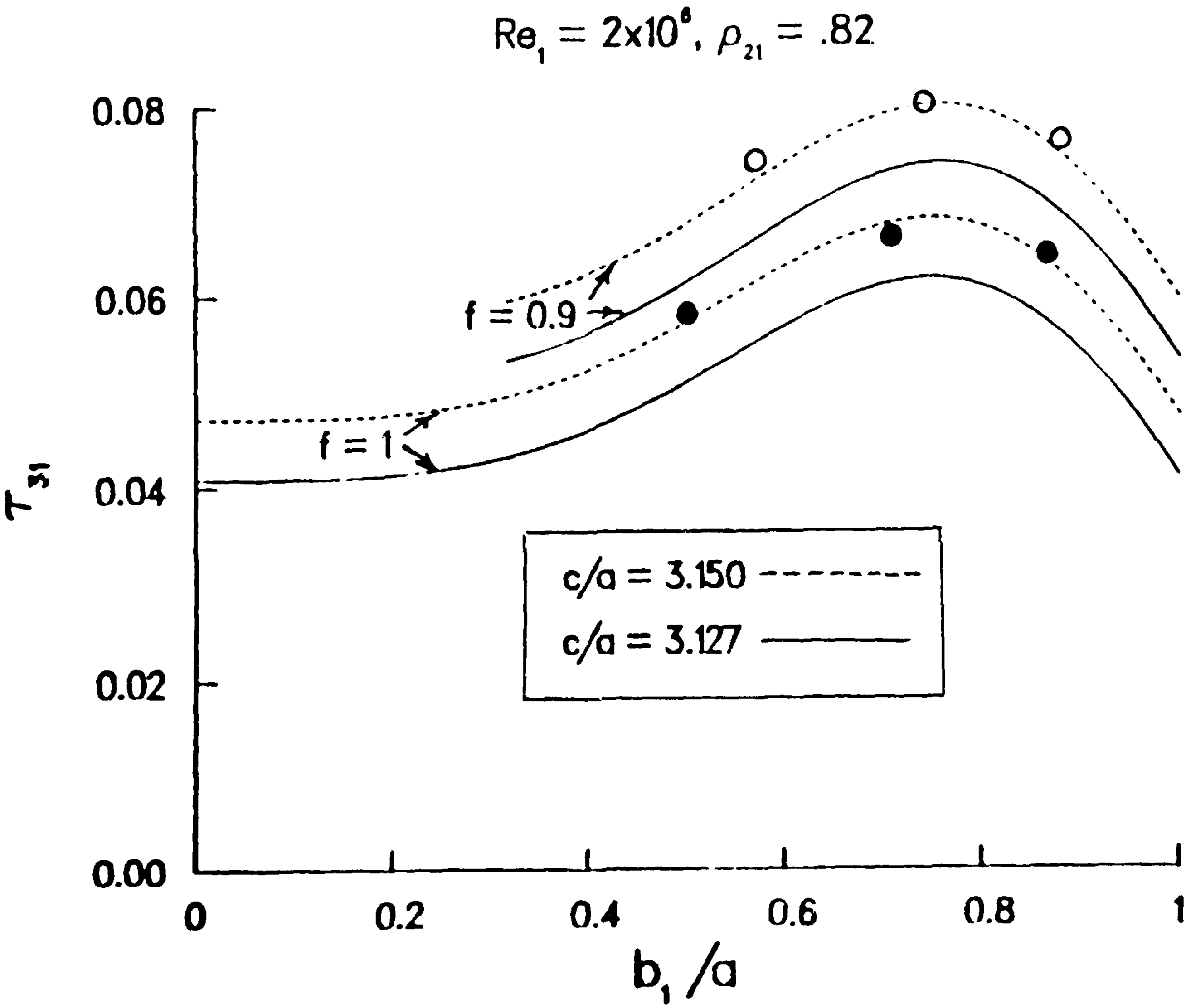

Figure 4. τ_{31} versus b_1/a for $Re_1 = 2 \times 10^6$, $c/a = 3.127$, $\rho_{21} = .82$ and Various Free Surface Fill Ratios. Experimental Data are from Reference 9.

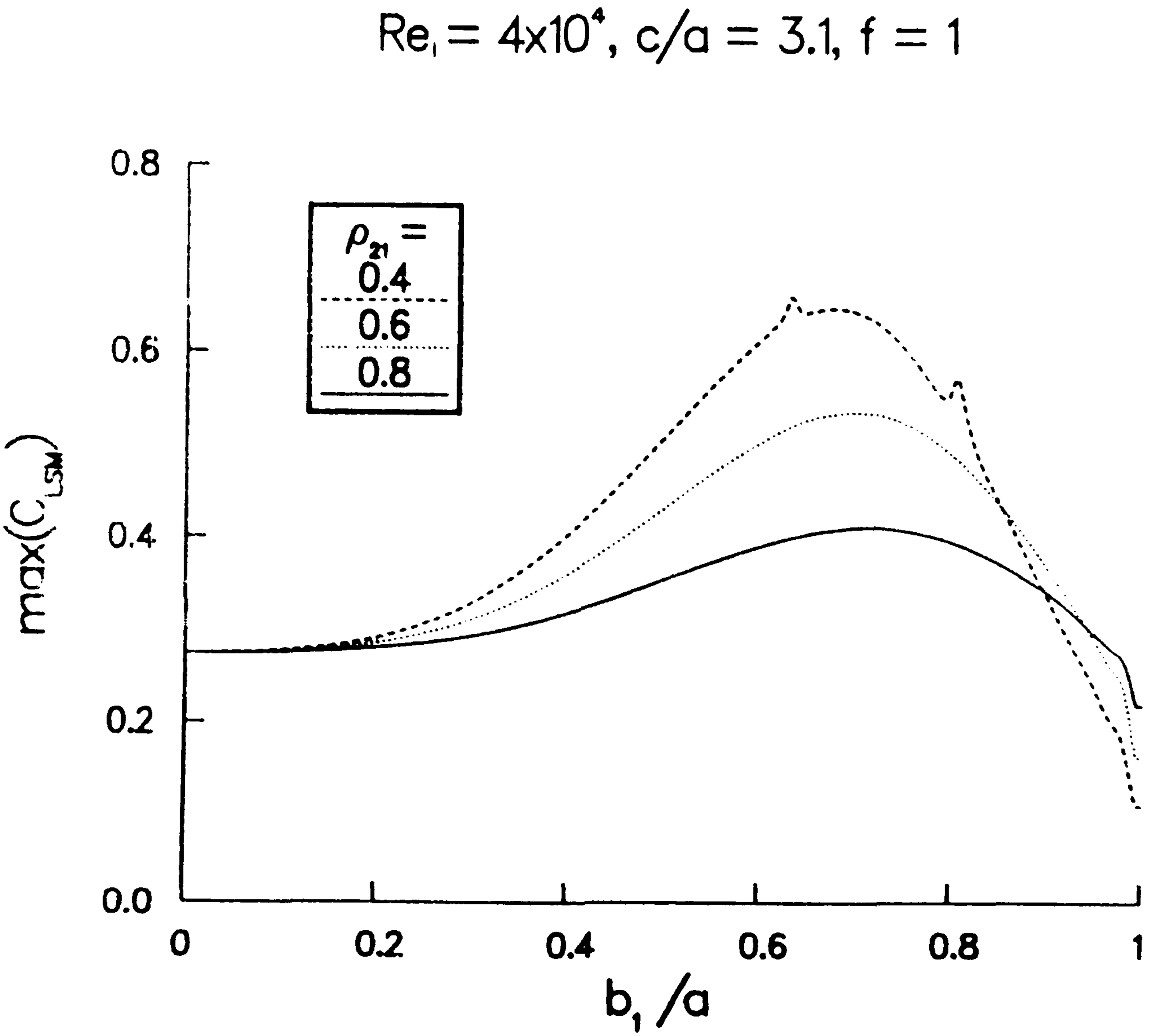

Figure 5. τ_{31} Maximum Side Moment Coefficient versus b_1/a for $Re_1 = 4 \times 10^4$, $c/a = 3.1$, $f = 1$ and Various Density Ratios.

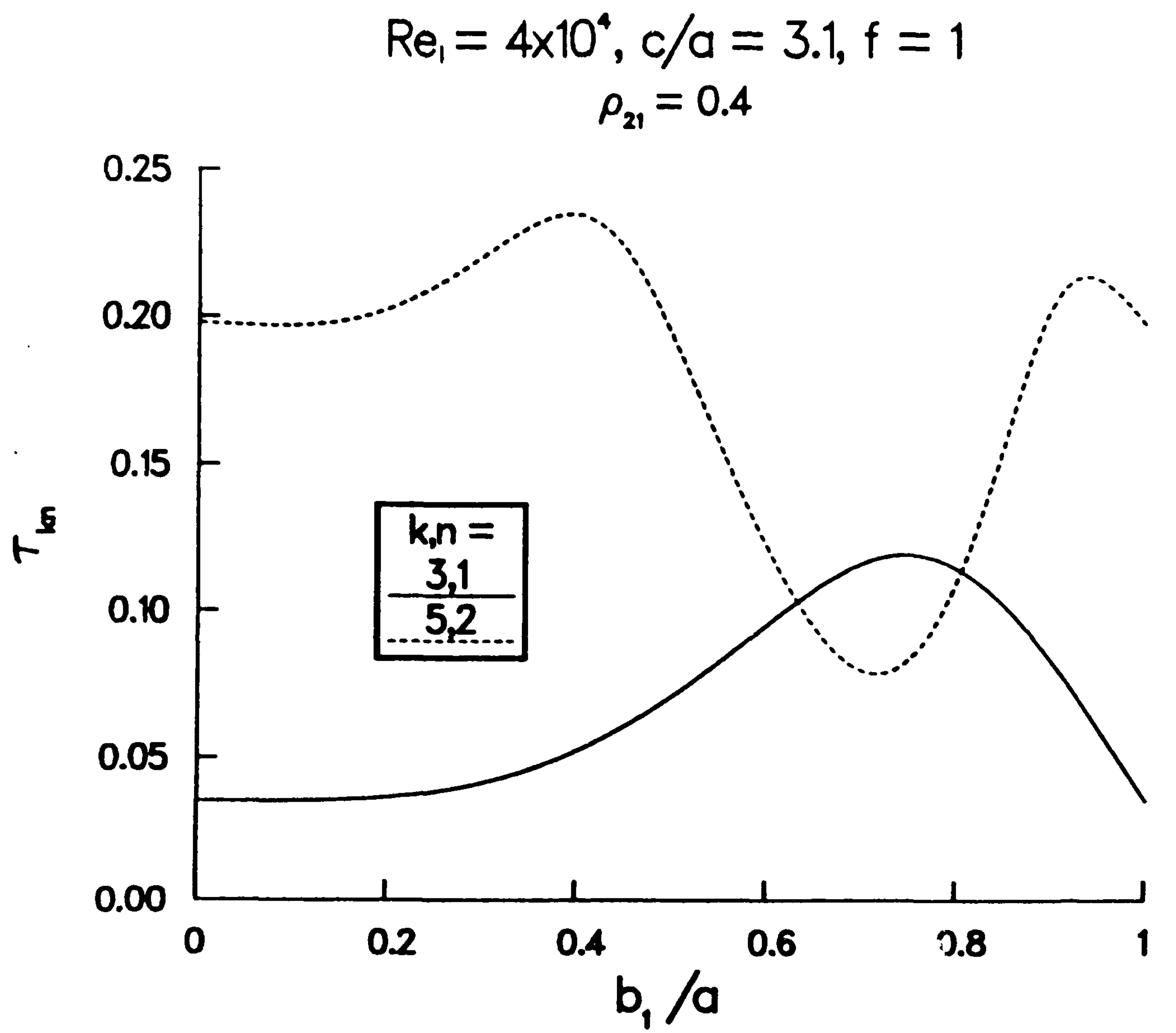

Figure 6. τ_{31} and τ_{52} versus b_1/a for $Re_1 = 4 \times 10^4$, $c/a = 3.1$, $f = 1$, $\rho_{21} = .4$.

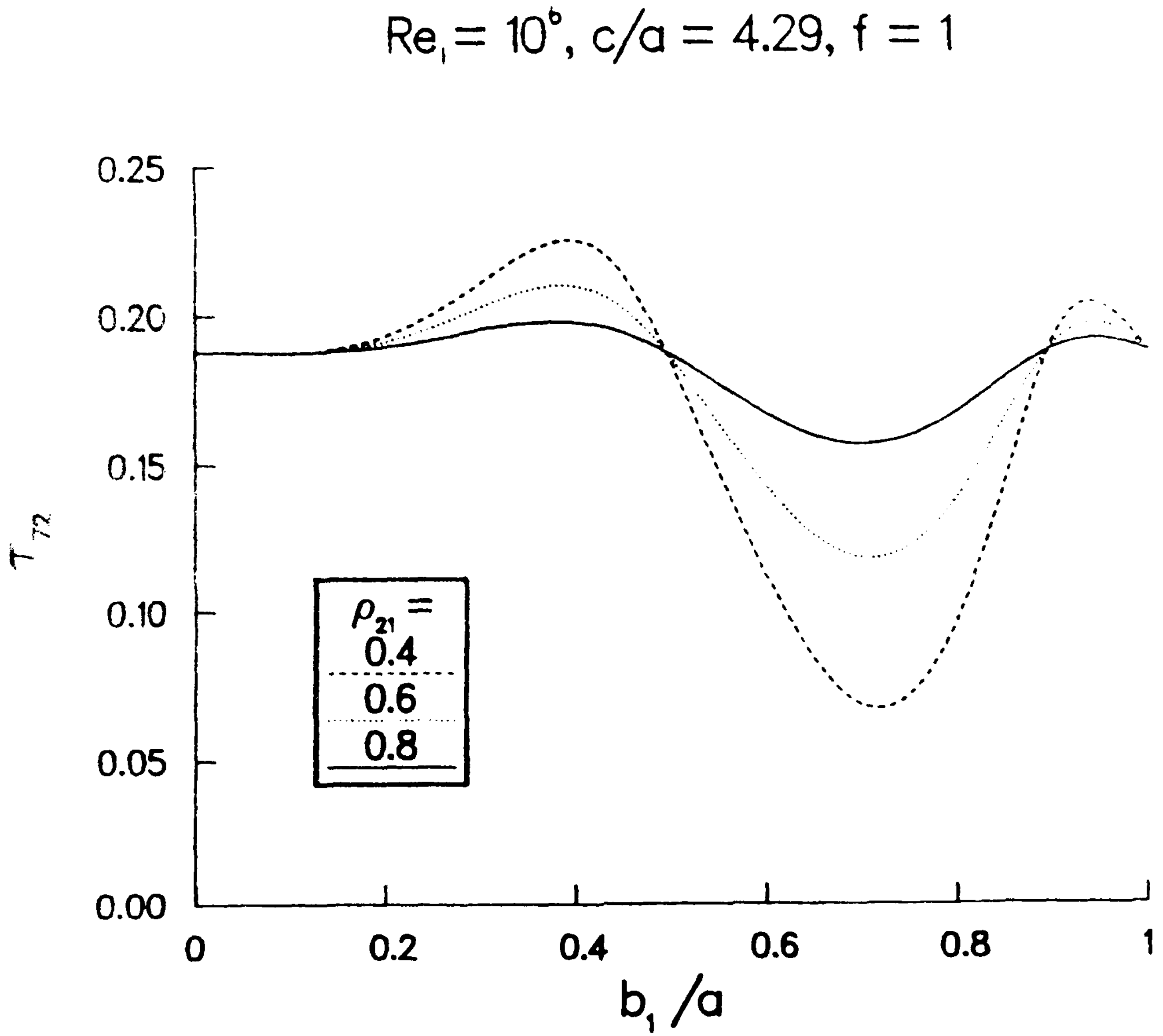

Figure 7. τ_{72} versus b_1/a for $Re_1 = 10^6$, c/a = 4.29, f = 1 and Various Density Ratios.

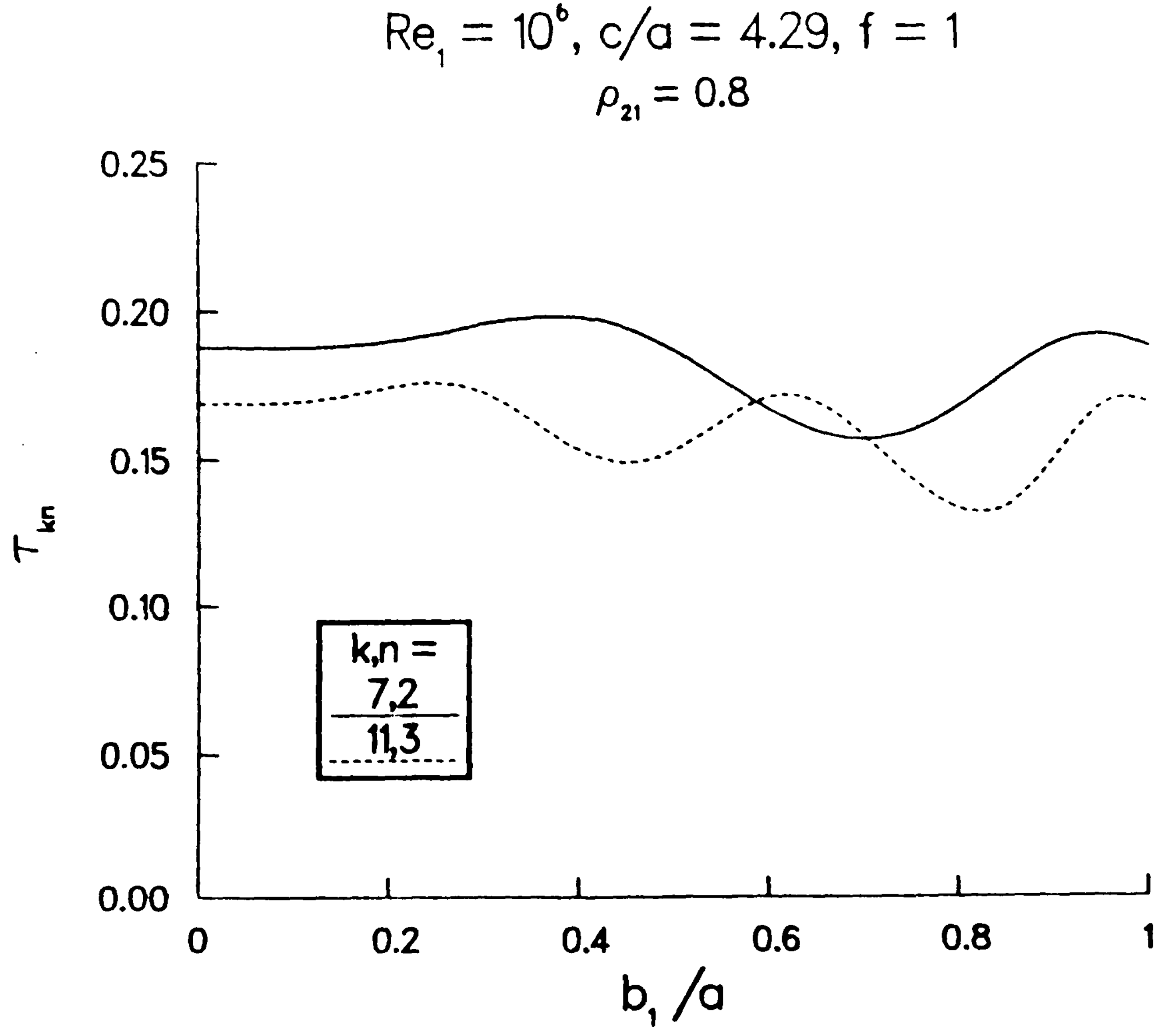

Figure 8. τ_{72} and $\tau_{11,3}$ versus b_1/a for $Re_1 = 10^6$, $c/a = 4.29$, $f = 1$ and $\rho_{21} = 0.8$.

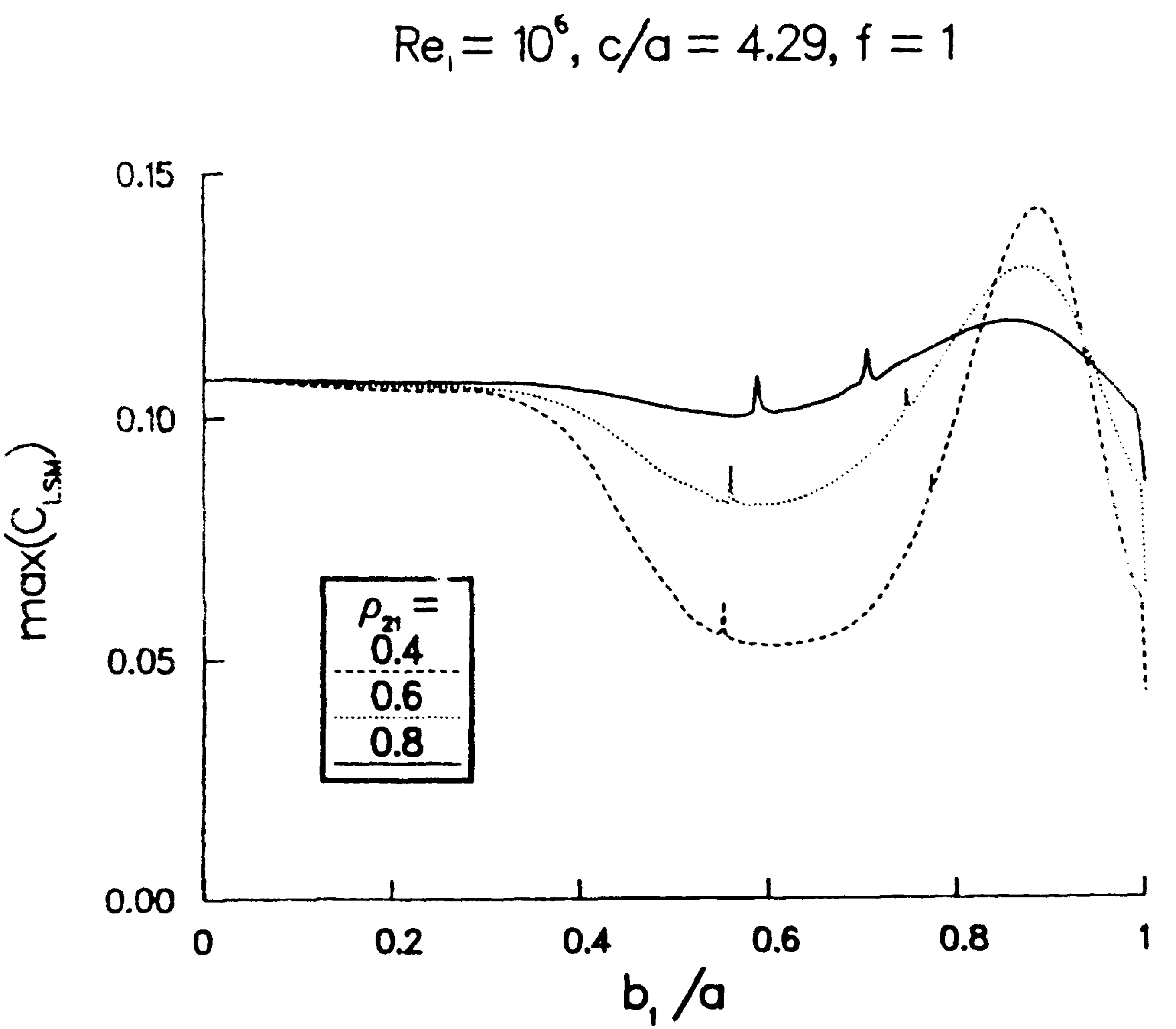

Figure 9. τ_{72} Maximum Side Moment Coefficient versus b_1/a for $Re_1 = 10^6$, $c/a = 4.29$, $f = 1$ and Various Density Ratios.

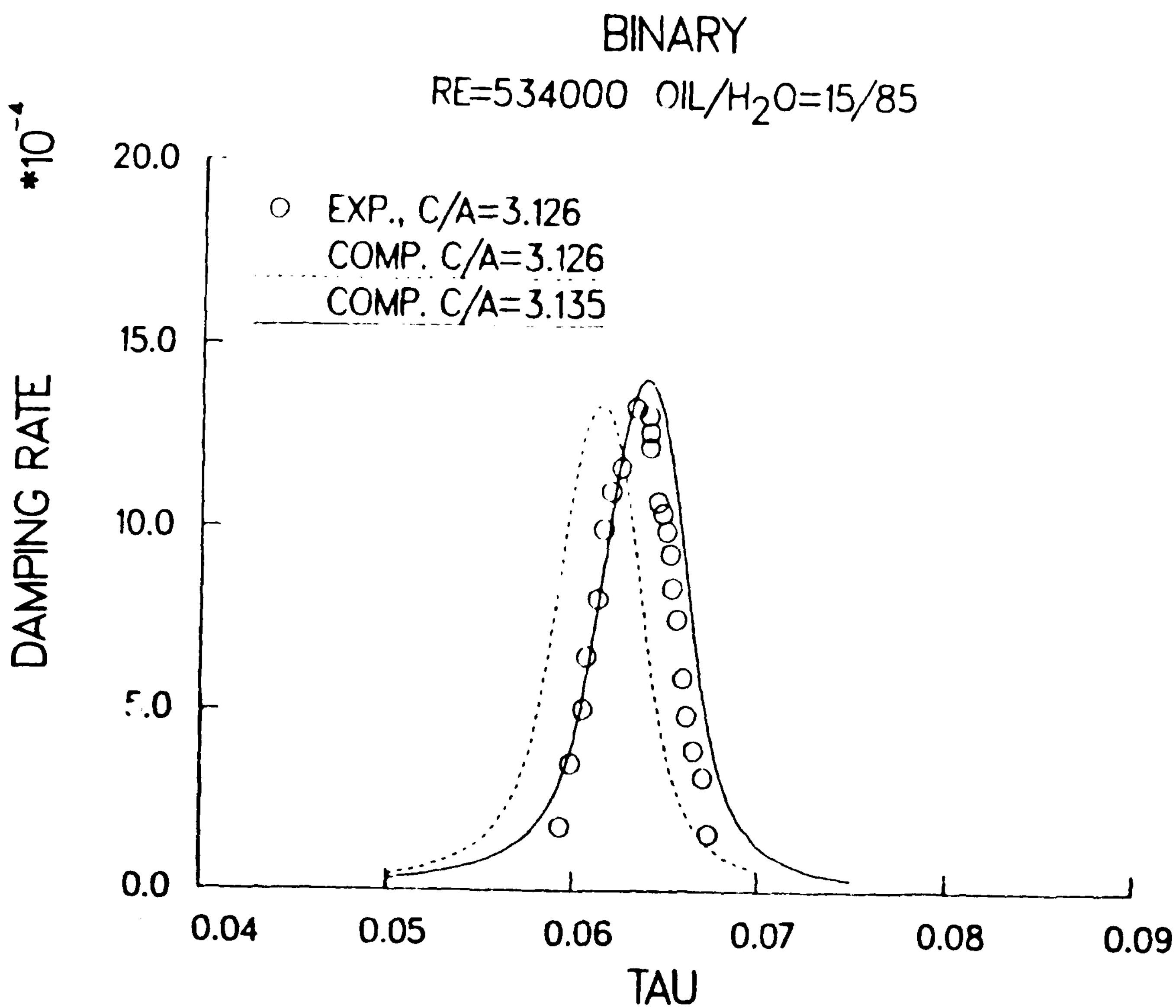

Figure 10. Damping Rate, $-\epsilon\tau$, versus τ for $Re_1 - 5.34 \times 10^5$, $f = .89$, $\rho_{21} = .812$.

REFERENCES

1. K. Stewartson, "On the [illegible] Spinning Top Containing Liquid," Journal of Fluid Mechanics, [illegible], September 1959, pp. 577-592.

2. E. H. Wedemeyer, "Viscous Correction to Stewartson's Stability Criterion," Ballistic Research Laboratory, Aberdeen Proving Ground, Maryland, BRL Report No. [illegible] 1966. [illegible]

3. C. H. Murphy, "Angular Motion of a Spinning Projectile With a Viscous Liquid Payload," Ballistic Research Laboratory, Aberdeen Proving Ground, Maryland, BRL Memorandum Report ARBRL-MR-03194, August 1982. (AD A118676). (See also Journal of Guidance, Control, and Dynamics, Vol. 6, July-August 1983, pp. 280-286.)

4. C. W. Kitchens, Jr., N. Gerber, and R. Sedney, "Oscillations of a Liquid in a Rotating Cylinder: Solid Body Rotation," Ballistic Research Laboratory, Aberdeen Proving Ground, Maryland, BRL Technical Report BRL-TR-02081, June 1978. (AD A057759)

5. N. Gerber, R. Sedney, and J. M. Bartos, "Pressure Moment on a Liquid-Filled Projectile: Solid Body Rotation," Ballistic Research Laboratory, Aberdeen Proving Ground, Maryland, BRL Technical Report ARBRL-TR-02422, October 1982. (AD A120567)

6. N. Gerber and R. Sedney, "Moment on a Liquid-Filled Spinning and Nutating Projectile: Solid Body Rotation," Ballistic Research Laboratory, Aberdeen Proving Ground, Maryland, BRL Technical Report ARBRL-TR-02470, February 1983. (AD A125332)

7. C. H. Murphy, "Liquid Payload Roll Moment Induced by a Spinning and Coning Projectile," Ballistic Research Laboratory, Aberdeen Proving Ground, Maryland, BRL Technical Report ARBRL-TR-02521, September 1983. (AD A133681) (See also AIAA Paper 83-2142, August 1983.)

8. C. H. Murphy, "A Relationship Between Liquid Roll Moment and Liquid Side Moment," Ballistic Research Laboratory, Aberdeen Proving Ground, Maryland, BRL Memorandum Report ARBRL-MR-03347, April 1984. (AD A140658)

9. W. E. Scott, "The Inertial Wave Frequency Spectrum in a Cylindrically Confined, Inviscid, Incompressible Two Component Liquid," Ballistic Research Laboratory, Aberdeen Proving Ground, Maryland, BRL Report No. 1609, September 1972. (AD 752439). (See also Physics of Fluids, Vol. 16, No. 1. pp. 9-12, January 1973.)

10. [illegible], "Flight Instabilities of Spinning Projectiles Having Non-Rigid Payloads," Journal of Guidance, Control, and Dynamics, Vol. 5, March-April 1982, pp. 151-157.

11. [illegible] and [illegible], "Flight Instability Produced by a Rapidly Spinning, Highly Viscous Liquid," Journal of Spacecraft and Rockets, Vol. [illegible], January-February [illegible], pp. [illegible].

REFERENCES (Continued)

12. W. P. D'Amico and W. H. Clay, "High Viscosity Liquid Payload Yawsonde Data for Small Launch Yaws," Ballistic Research Laboratory, Aberdeen Proving Ground, Maryland, BRL Memorandum Report ARBRL-MR-03029, June 1980. (AD A088411)

13. L. D. Kayser, W. P. D'Amico, and W. I. Brannan, "Free Gyroscope Experiments Involving Two Immiscible Liquids in a Partially-Filled Container," Ballistic Research Laboratory, Aberdeen Proving Ground, Maryland, BRL Memorandum Report in preparation.

A1. J. T. Frasier and W. E. Scott, "Dynamics of a Liquid-Filled Shell: Cylindrical Cavity with a Central Rod," Ballistic Research Laboratory, Aberdeen Proving Ground, Maryland, BRL Memorandum Report BRL-MR-1391, February 1968. (AD 667365)

A2. J. T. Frasier, "Dynamics of a Liquid-Filled Shell: Viscous Effects in a Cylindrical Cavity with a Central Rod," Ballistic Research Laboratory, Aberdeen Proving Ground, Maryland, BRL Memorandum Report BRL-MR-1959, January 1969. (AD 684344)

C1. K. D. Aldridge, "Experimental Verification of the Inertia Oscillations of a Liquid in a Cylinder During Spinup," BRL Contract Report 273, September 1975. (AD A0187970) (See also Geophys. Astrophys. Fluid Dynamics, Vol. 8, 1977, pp. 279-301.)

C2. C. H. Murphy, "Moment Induced by Liquid Payload During Spin-Up Without a Critical Layer," Ballistic Research Laboratory, Aberdeen Proving Ground, Maryland, BRL Technical Report ARBRL-TR-02581, August 1984. (AD A145716)

APPENDIX A

EFFECT OF CENTRAL ROD

APPENDIX A. EFFECT OF CENTRAL ROD

The effect of a central rod on a single liquid payload has been discussed in detail by Frasier.[A1-A2] Conditions (2.19 - 2.21) at $r = b_2$ are replaced by conditions similar to (2.22 - 2.24).

$$u_{2s}(b_2,x) = (s - i)\ (b_2/a)\ \hat{K}\ . \tag{A1}$$

$$v_{2s}(b_2,x) = -(s - i)\ (x/a)\ \hat{K}\ . \tag{A2}$$

$$w_{2s}(b_2,x) = i(s - i)\ (x/a)\ \hat{K}. \tag{A3}$$

Equation (A2), of course, replaces Eq. (5.3) as the boundary condition at $r = b_2$. Eqs. (4.16 - 4.17) are then replaced by

$$w_{2si}(b_2,x) + w_{21}\varepsilon_2 + w_{22} = i\ (s-i)\ \hat{K}(x/a) \tag{A4}$$

$$u_{2si}(b_2,x) + u_{21}\varepsilon_2 + u_{22} = (s-i)\ \hat{K}(b_2/a)\ . \tag{A5}$$

A revised version of Table 2 can be computed for the viscous coefficient functions (see Table A1). For these viscous coefficient functions the only radial viscous velocity to be affected is that at $r = b_2$ [Eq. (4.25)].

$$v_{2sv}(b_2,x) = (a/b_2)\ (v_{22} + \varepsilon_2\ v_{21})\ \delta_{a2}\ . \tag{A6}$$

The inviscid boundary conditions now differ from Eqs. (5.1 - 5.4) by the condition at $r = b_2$. They are

at $r = b_1$

$$p_{1si} + \frac{b_1\ v_{1si}}{a\ (s - i)} = \rho_{21}\left[p_{2si} + \frac{b_1\ v_{2si}}{a\ (s - i)}\right] \tag{A7}$$

A1. J. T. Frasier and W. W. Scott, "Dynamics of a Liquid-Filled Shell: Cylindrical Cavity with a Central Rod," Ballistic Research Laboratory, Aberdeen Proving Ground, Maryland, BRL Memorandum Report BRL-MR-1391, [illegible]

A2. [illegible], "Dynamics of a Liquid-Filled Shell: Viscous Effects in a Cylindrical Cavity with a Central Rod," Ballistic Research Laboratory, Aberdeen Proving Ground, Maryland, BRL Memorandum Report BRL-MR-1959, [illegible]

TABLE A1. VISCOUS COEFFICIENT FUNCTIONS FOR CENTRAL ROD.

$$w_{10} = \{[1+N - (1-N)\ \varepsilon_2^{\,2}]\ w_a + N\ \varepsilon_1\ \Delta\ w_{si}\}\hat{D}^{-1}$$

$$w_{11} = \{(1-N)\ \varepsilon_1 w_a - N(1+\varepsilon_2^{\,2})\Delta\ w_{si} + 2\ N\ \varepsilon_2 w_b\}\hat{D}^{-1}$$

$$w_{21} = \{2\ \varepsilon_1 w_a + (1+\varepsilon_1^{\,2})\Delta\ w_{si} - \varepsilon_2(1-N)\ w_b\}\hat{D}^{-1}$$

$$w_{22} = \{-\varepsilon_2\ \Delta\ w_{si} + \{[1+N + (1-N)\ \varepsilon_1^{\,2}]\ w_b\}\ \hat{D}^{-1}$$

$$u_{10} = \{[1+N - (1-N)\ \varepsilon_2^{\,2}]\ u_a + N\ \varepsilon_1\ \Delta\ u_{si}\}\ \hat{D}^{-1}$$

$$u_{11} = \{(1-N)\ \varepsilon_1 u_a - N\ (1+\varepsilon_2^{\,2})\ \Delta\ u_{si} + 2\ N\ \varepsilon_2\ u_b\}\hat{D}^{-1}$$

$$u_{21} = \{2\ \varepsilon_1 u_a + (1+\varepsilon_1^{\,2})\ \Delta\ u_{si} - \varepsilon_2\ (1-N)\ u_b\}\hat{D}^{-1}$$

$$u_{22} = \{-\varepsilon_2\ \Delta\ u_{si} + [1+N + (1-N)\ \varepsilon_1^{\,2}]\ u_b\}\hat{D}^{-1}$$

$$v_{10} = \{[1+N - (1-N)\ \varepsilon_2^{\,2}]\ v_a + N\ \varepsilon_1 \Delta^*\}\hat{D}^{-1}$$

$$v_{11} = \{-(1-N)\ \varepsilon_1 v_a + N(1+\varepsilon_2^{\,2})\ \Delta^* - 2\ N\ \varepsilon_2 v_b\}\hat{D}^{-1}$$

$$v_{21} = \{2\ \varepsilon_1 v_a + (1+\varepsilon_1^{\,2})\ \Delta^* - \varepsilon_2(1-N)\ v_b\}\hat{D}^{-1}$$

$$v_{22} = \{\varepsilon_2\ \Delta^* - [1+N + (1-N)\ \varepsilon_1^{\,2}]\ v_b\}\hat{D}^{-1}$$

---

where

$$\hat{D} = 1 + N + (1 - N)\ (\varepsilon_1^{\,2} - \varepsilon_2^{\,2})$$

$$w_b = i\ (s - i)\ (x/a)\ \hat{K} - w_{2si}(b_2, x)$$

$$u_b = (s - i)\ (b_2/a)\ \hat{K} - u_{2si}(b_2/x)$$

$$v_b = -(s - i)\ (x/a)\ \hat{K} - \left[\frac{\partial\ (r\ v_{2si})}{\partial r}\right]_{r\ =\ b_2}$$

$$v_{1si} = v_{2si} + (1 - \rho_{21})\, v_{2sv} \tag{A8}$$

at $r = b_2$

$$v_{2si} + v_{2sv} = (i - s)\,(x/a)\,\hat{K} \tag{A9}$$

at $r = a$

$$v_{1si} + v_{1sv} = (i - s)\,(x/a)\,\hat{K}, \tag{A10}$$

where the necessary viscous coefficient functions v_{jk} are given in Table A1.

It should be noted that in terms of δ_{aj} the computational versions of Eqs. (A9-A10) which are used in this paper are slightly more accurate than those of Reference 3. For a single liquid they become

$$v_{si}\,(b_2,x) + \left[\frac{b_2 a\delta_a}{b_2 + a\delta_a}\right] \frac{\partial\, v_{si}(b_2,x)}{\partial r} = (i - s)\,(x/a)\,\hat{K} \tag{A11}$$

$$v_{si}\,(a,x) - \left[\frac{a\delta_a}{1-\delta_a}\right] \frac{\partial\, v_{si}(a,x)}{\partial r} = (i - s)\,(x/a)\,\hat{K}\,. \tag{A12}$$

The corresponding equations of Reference 3 are:

$$v_{si}\,(b_2,x) + a\delta_a \frac{\partial\, v_{si}(b_2,x)}{\partial r} = (i - s)\,(x/a)\,\hat{K} \tag{A13}$$

$$v_{si}\,(a,x) - a\delta_a \frac{\partial\, v_{si}(a,x)}{\partial r} = (i - s)\,(x/a)\,\hat{K}. \tag{A14}$$

The difference between Eqs. (A11) and (A13) is only important when b_2 is very small while the difference between Eqs. (A12) and (A14) is unimportant for Reynolds numbers appropriate to boundary layer theory.

After the usual substitutions of the Fourier series expansions, new forms of Eqs. (5.5 - 5.9) for the E_{jk}'s and F_{jk}'s can be obtained.

$$R_{1k}(b_1) - \rho_{21} R_{2k}(b_1) - (b_1/a)\ (s - i)^{-1} [R_{v1k}(b_1) - \rho_{21} R_{v2k}(b_1)]$$

$$= \frac{(1 - \rho_{21})\ s^2\ (i - s)}{i + s} (b_1/a)\ a_k \tag{A15}$$

$$R_{v1k}(b_1) - R_{v2k}(b_1) - (1 - \rho_{21})\ \delta_{a2}\ \hat{R}_k^{*} = (1 - \rho_{21})(\varepsilon_1 - \varepsilon_2)\ \delta_{a2}\ \hat{A}_1 a_k \tag{A16}$$

$$R_{v2k}(b_2) + a\ \delta_{a2}\ D\ \hat{D}_2^{-1}\ R'_{v2k}(b_2) + (a/b_2)\ \varepsilon_2\ \delta_{a2}\ \hat{D}_2^{-1}\ R_k^{**}$$

$$= \frac{2s\ (i - s)}{i + s} a_k \tag{A17}$$

$$R_{v1k}(a) - a\ \delta_{a1}\ \hat{A}_2\ R'_{v1k}\ (a) + \varepsilon_1\ \delta_{a1}\ N\ \hat{D}_0^{-1}\ R_k^{**} = \frac{2s\ (i - s)}{i + s}\ a_k\ , \tag{A18}$$

where

$$\hat{R}_k^{*} = \{a\ (1 + \varepsilon_1^{\,2} + \varepsilon_2^{\,2})\ [R'_{v1k}(b_1) - R'_{v2k}(b_1)]$$

$$- 2\ (a/b_1)\ \varepsilon_1\ [R_{v1k}(a) + a\ R'_{v1k}(a)]$$

$$+ 2\ (a/b_1)\ \varepsilon_2\ [R_{v2k}(b_2) + b_2\ R'_{v2k}(b_2)]\}\ \hat{D}_1^{-1}$$

$$\hat{A}_1 = 4\ (a/b_1)\ [\frac{s\ (i - s)}{i + s}]\ \hat{D}_1^{-1}$$

$$\hat{A}_2 = [1 + N - (1 - N)(\varepsilon_1^{\,2} + \varepsilon_2^{\,2})]\ \hat{D}_0^{-1}$$

$$\hat{D}_0 = \hat{D} - \delta_{a1}\ [1+N - (1-N)(\varepsilon_1^{\,2} + \varepsilon_2^{\,2})]$$

$$\hat{D}_1 = \hat{D} - \delta_{a2}\,(1-\rho_{21})(1+\varepsilon_1^{\,2}+\varepsilon_2^{\,2})(a/b_1)$$

$$\hat{D}_2 = \hat{D} + \delta_{a2}\,D\,(a/b_2).$$

The linear liquid moment coefficient for a cylinder with a central rod can be expressed as the sum of six terms--the four terms of Eq. (6.2) plus the pressure and viscous contributions from the central rod.

$$\tau\,(C_{LSM} + i\,C_{LIM}) = m_{p\ell} + m_{pe} + m_{pr} + m_{v\ell} + m_{ve} + m_{vr}\,. \tag{A19}$$

The two additional terms are quite similar to $m_{p\ell}$ and $m_{v\ell}$, respectively.

$$m_{pr} = -i\,b_2\,\rho_{21}\,(2a^2c\hat{K})^{-1}\int_{-c}^{c}\tilde{x}\,[\tilde{p}_{2si}(b_2,\tilde{x}) + p_{2sv}(b_2,\tilde{x})]\,d\tilde{x}\,, \tag{A20}$$

where $\quad p_{2sv} = -2\,\delta_{a2}\,(w_{22} - w_{21}\,\varepsilon_2).$

$$m_{vr} = N\,b_2\,(2\,a^2c\hat{K}\,R_{e1}\,\delta_{a1})^{-1}\int_{-c}^{c}[i\,b_2\,(u_{22}-\varepsilon_2 u_{21}) + \tilde{x}\,(w_{22}-\varepsilon_2\,w_{21})]\,d\tilde{x}\,. \tag{A21}$$

In Figure A1 the maximum side moment coefficient associated with τ_{31} is plotted versus b_1/a for the central rod of Figure 3. Note the sharp changes in side moment for the interface near the central rod and near the outer cylindrical wall. The two bumps in the $\rho_{21} = .4$ curve are caused by the coalescence of the τ_{31} and the τ_{52} eigenfrequencies.

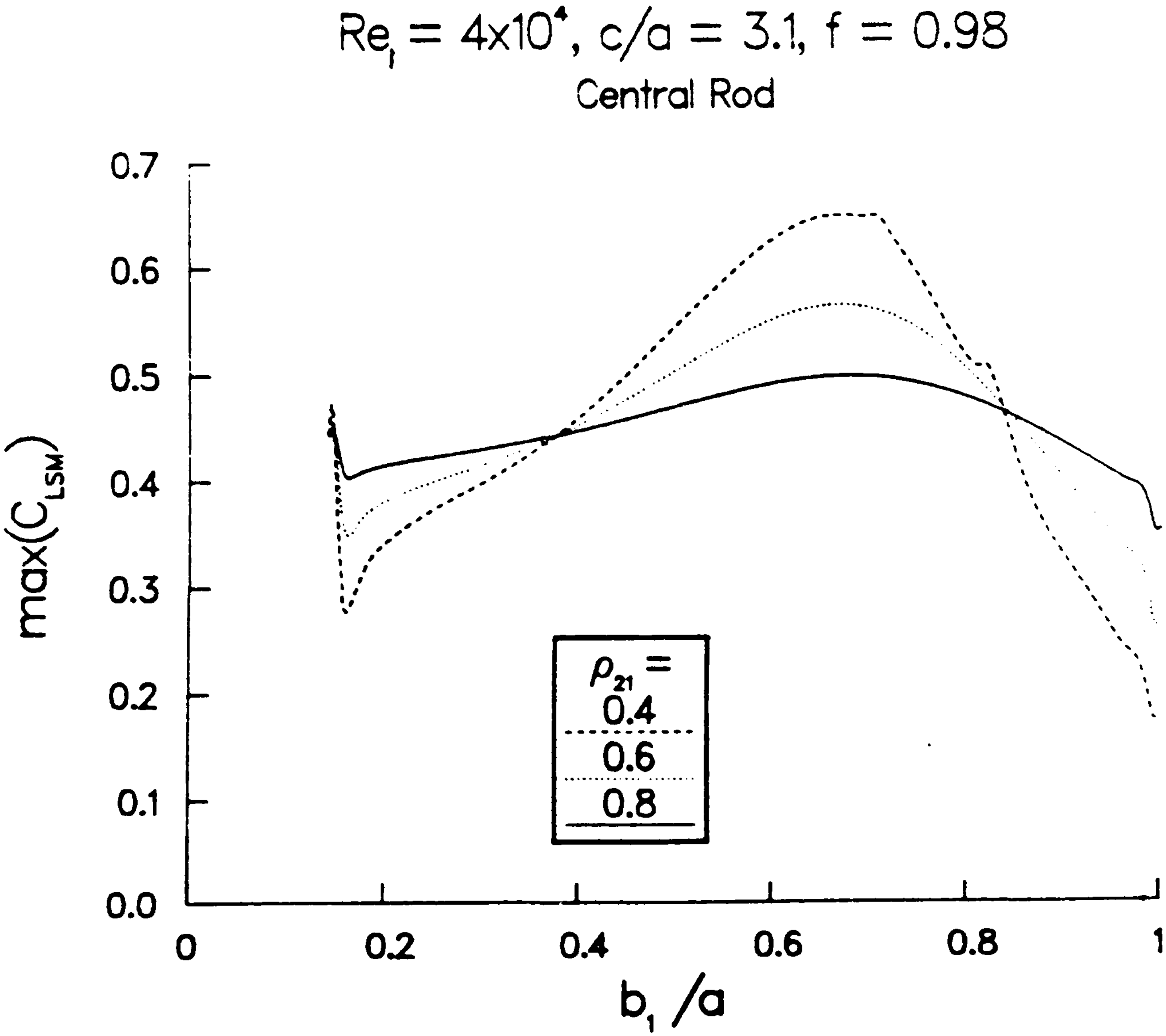

Figure A1. τ_{31} Maximum Side Moment Coefficient versus b_1/a for $Re_1 = 4 \times 10^4$, $c/a = 3.1$, $f = .98$ with a Central Rod and Various Density Ratios.

APPENDIX B

EFFECT OF DIFFERENT KINEMATIC VISCOSITIES

APPENDIX B. EFFECT OF DIFFERENT KINEMATIC VISCOSITIES

As was stated in the body of this report, the approximation given in Eq. (3.5) can be avoided by a much better least squares approximation. Exact expressions for p_{jsi}, v_{jsi}, and v_{jsv} can be derived from the series of Table 1 and the other relations given in the main part of this report, and these are tabulated in Table B1. Next, these expressions for the pressure and radial velocity perturbation functions are substituted in Eqs. (5.1-5.4) to obtain four equations for the E_{kj}'s and F_{kj}'s:

$$\sum_k [E_{1k} A_{\ell k} + F_{1k} B_{\ell k}] \sin(\lambda_{1k} x/c) + \sum_k [E_{2k} C_{\ell k} + F_{2k} D_{\ell k}] \sin(\lambda_{2k} x/c)$$

$$= d_\ell x/c \qquad \ell = 1,2,3,4 \qquad \text{(B1)}$$

$$k = 1,3,5,7,\ldots 2N_k - 1$$

where the coefficients $A_{\ell k}$, $B_{\ell k}$, $C_{\ell k}$, $D_{\ell k}$, d_ℓ are given in Table B2.

For N_k sets of the parameters (E_{1k}, E_{2k}, F_{1k}, F_{2k}), these four equations can not be satisfied exactly. We can, however, consider the squared sum of the residuals for each equation produced by a particular selection:

$$R_\ell^2 = \int_{-c}^{c} \Big| \sum [E_{1k} A_{\ell k} + F_{1k} B_{\ell k}] \sin(\lambda_{1k} x/c)$$

$$+ \sum [E_{2k} C_{\ell k} + F_{2k} D_{\ell k}] \sin(\lambda_{2k} x/c) - d_\ell x/c \Big|^2 dx. \qquad \text{(B2)}$$

We seek those values of the parameters E_{1k}, E_{2k}, F_{1k}, F_{2k} that minimize (in a least squares sense) the R_ℓ's. For a single liquid and 100% fill ($b_2 = 0$), the F_k's satisfy the condition at $r = b_2$ while the E_k's satisfy the condition at $r = a$. For two liquids, the conditions at b_2 and a are represented in Eqs. (B1-B2) by $\ell = 3$ and 4, respectively. Hence, in analogy with the simpler case, we select the F_{2k}'s to minimize R_3 and the E_{1k}'s to minimize R_4. To satisfy the interface conditions ($\ell = 1,2$), we select the F_{1k}'s to minimize R_1 and the E_{2k}'s to minimize R_2. The resulting $4N_k$ equations are given in Table B3.

Tables B1 and B2 have to be modified for a fully-filled cylinder with a central rod of radius b_2. The pressure and inviscid radial velocity functions

in Table B1 are unchanged, but three viscous radial velocity functions have to be derived from Table A1 and are given in Table B4.

As was indicated in Appendix A, the boundary conditions at $r = b_2$ for the free surface (Eq. (5.3)) is replaced by Eq. (A3). The corresponding Eq. (B1) is identified by $\ell = 3$. The new coefficients are:

$$
\begin{aligned}
A_{3\kappa} &= (a/b_2)\ \delta_{a2}\ h^*_{1\kappa} \\
B_{3\kappa} &= (a/b_2)\ \delta_{a2}\ h^*_{2\kappa} \\
C_{3\kappa} &= f_{2\kappa}\ (b_2) + (a/b_2)\ \delta_{a2}\ h^*_{3k} \\
D_{3\kappa} &= g_{2k}\ (b_2) + (a/b_2)\ \delta_{a2}\ h^*_{4k} \\
d_3 &= 2\ s(i - s)\ (i + s)^{-1} - (a/b_2)\ \delta_{a2}\ h^*_1 .
\end{aligned}
\tag{B4}
$$

The remaining coefficients for $\ell = 1,2,4$ are given in Table B3 when the h_n, $h_{n\kappa}$'s of Table B4 are used.

As a comparison of approximation (Eq. 3.5) with the better approximation of this appendix, the maximum side moment coefficient for τ_{31}, Re = 40,000, $c/a = 3.1$, $b_2 = 0$, $\rho = 0.6$ is plotted versus b_1/a in Figure B1. Comparison of the two approximations are given for kinematic viscosity ratios ($\nu_{21} = \nu_2/\nu_1$) of 0.1, 1, and 10. We see that approximation (Eq. 3.5) underestimates the effect of unequal kinematic viscosities.

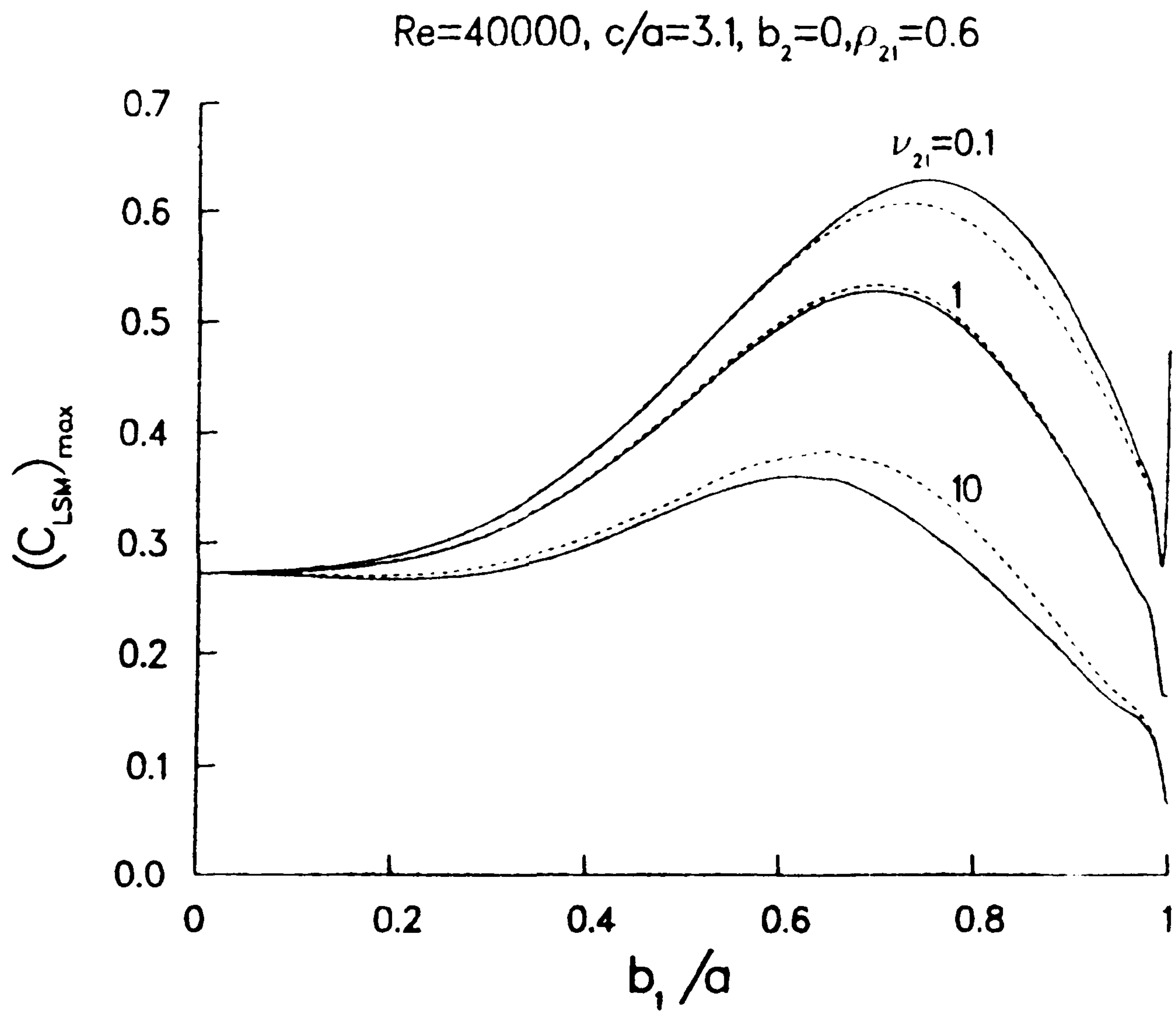

Figure B1. τ_{31} Maximum Side Moment Coefficient versus b_1/a for $Re_1 = 4 \times 10^4$, $c/a = 3.1$, $f = .98$, $\rho_{21} = .6$ and Various Kinematic Viscosity Ratios. Using Average Viscosities Produces the Dashed Curves.

TABLE B1. PRESSURE AND RADIAL VELOCITY FUNCTIONS.

$$p_{jsi} = -\{(i-s)^2 (x/c)(r/a) + \Sigma\,[E_{jk} J_{1k}(\hat{r}) + F_{jk} Y_{1k}(\hat{r})] \sin(\lambda_{jk} x/c)\}\,(c/a)\,\hat{K}$$

$$v_{jsi} = \{(i-s)^2 (i+s)^{-1} (x/c) + \Sigma\,[E_{jk} f_{jk}(r) + F_{jk} g_{jk}(r)] \sin(\lambda_{jk} x/c)\}\,(c/a)\,\hat{K}$$

$$v_{1sv}(a,x) = \{h_1 x/c + \Sigma\,[E_{1k}\, h_{1k} + F_{1k}\, h_{2k}] \sin(\lambda_{1k} x/c)$$

$$+ \Sigma\,[E_{2k}\, h_{3k} + F_{2k}\, h_{4k}] \sin(\lambda_{2k} x/c)\}\,(c/a)\,\delta_{a1}\,\hat{K}$$

$$v_{2sv}(b_1,x) = \{h_2 x/c + \Sigma\,[E_{1k}\, h_{5k} + F_{1k}\, h_{6k}] \sin(\lambda_{1k} x/c)$$

$$+ \Sigma\,[E_{2k}\, h_{7k} + F_{2k}\, h_{8k}] \sin(\lambda_{2k} x/c)\}\,(c/b_1)\,\delta_{a2}\,\hat{K}$$

where

$$\hat{r} = \hat{\lambda}_{jk}\, r/c$$

$$f_{jk}(r) = -[(i-s)\,(a/c)\,\hat{\lambda}_{jk} \frac{dJ_1(\hat{r})}{d\hat{r}} + 2i\,(a/r)\,J_1\,(\hat{r})]\,S^{-1}$$

$$g_{jk}(r) = -[(i-s)\,(a/c)\,\hat{\lambda}_{jk} \frac{dY_1(\hat{r})}{d\hat{r}} + 2i\,(a/r)\,Y_1\,(\hat{r})]\,S^{-1}$$

$$h_1 = 2s\,[1 - 2\varepsilon_1^{\,2}\,(1 - N)\,D^{-1}]\,(i-s)\,(i+s)^{-1}$$

$$h_2 = 4\,\varepsilon_1\,s\,(i-s)\,(i+s)^{-1}\,D^{-1}$$

$$h_{1k} = -[1 - 2\,\varepsilon_1^{\,2}\,(1 - N)\,D^{-1}]\,\hat{f}_{1k}(a) + 2\,\varepsilon_1\,N\,D^{-1}\,\hat{f}_{1k}(b_1)$$

$$h_{2k} = -[1 - 2\,\varepsilon_1^{\,2}\,(1 - N)\,D^{-1}]\,\hat{g}_{1k}(a) + 2\,\varepsilon_1\,N\,D^{-1}\,\hat{g}_{1k}\,(b_1)$$

TABLE B1. PRESSURE AND RADIAL VELOCITY FUNCTIONS (Continued).

$$h_{3k} = -2\ \varepsilon_1\ N\ D^{-1}\ \hat{f}_{2k}\ (b_1)$$

$$h_{4k} = -2\ \varepsilon_1\ N\ D^{-1}\ \hat{g}_{2k}\ (b_1)$$

$$h_{5k} = -2\ \varepsilon_1\ D^{-1}\ \hat{f}_{1k}\ (a) + (1 + \varepsilon_1^{\ 2} - \varepsilon_2^{\ 2})\ D^{-1}\ \hat{f}_{1k}\ (b_1)$$

$$h_{6k} = -2\ \varepsilon_1\ D^{-1}\ \hat{g}_{1k}\ (a) + (1 + \varepsilon_1^{\ 2} - \varepsilon_2^{\ 2})\ D^{-1}\ \hat{g}_{1k}\ (b_1)$$

$$h_{7k} = -(1 + \varepsilon_1^{\ 2} - \varepsilon_2^{\ 2})\ D^{-1}\ \hat{f}_{2k}\ (b_1)$$

$$h_{8k} = -(1 + \varepsilon_1^{\ 2} - \varepsilon_2^{\ 2})\ D^{-1}\ \hat{g}_{2k}\ (b_1)$$

$$\hat{f}_{jk} = f_{jk} + r\ f'_{jk}$$

$$\hat{g}_{jk} = g_{jk} + r\ g'_{jk}$$

TABLE B2. COEFFICIENTS OF EQ. (B1).

$$A_{1k} = J_1 (\hat{\lambda}_{1k} b_1/c) + (b_1/a) (i-s)^{-1} f_{1k} (b_1)$$

$$B_{1k} = Y_1 (\hat{\lambda}_{1k} b_1/c) + (b_1/a) (i-s)^{-1} g_{1k} (b_1)$$

$$C_{1k} = -\rho_{21} [J_1(\hat{\lambda}_{2k} b_1/c) + (b_1/a) (i-s)^{-1} f_{2k} (b_1)]$$

$$D_{1k} = -\rho_{21} [Y_1(\hat{\lambda}_{2k} b_1/c) + (b_1/a) (i-s)^{-1} g_{2k} (b_1)]$$

$$A_{2k} = (b_1/a) f_{1k} (b_1) - (1 - \rho_{21}) \delta_{a2} h_{5k}$$

$$B_{2k} = (b_1/a) g_{1k} (b_1) - (1 - \rho_{21}) \delta_{a2} h_{6k}$$

$$C_{2k} = -(b_1/a) f_{2k} (b_1) - (1 - \rho_{21}) \delta_{a2} h_{7k}$$

$$D_{2k} = -(b_1/a) g_{2k} (b_1) - (1 - \rho_{21}) \delta_{a2} h_{8k}$$

$$A_{3k} = B_{3k} = 0$$

$$C_{3k} = J_1(\hat{\lambda}_{2k} b_2/c) + (b_2/a) (i-s)^{-1} f_{2k} (b_2)$$

$$D_{3k} = Y_1(\hat{\lambda}_{2k} b_2/c) + (b_2/a) (i-s)^{-1} g_{2k} (b_2)$$

$$A_{4k} = f_{1k}(a) + \delta_{a1} h_{1k}$$

$$B_{4k} = g_{1k} (a) + \delta_{a1} h_{2k}$$

$$C_{4k} = \delta_{a1} h_{3k}; \qquad D_{4k} = \delta_{a1} h_{4k}$$

$$d_1 = 0$$

$$d_2 = (1 - \rho_{21}) \delta_{a2} h_2$$

$$d_3 = s^2 (i - s) (i + s)^{-1} (b_2/a)$$

$$d_4 = 2s (i - s) (i + s)^{-1} - \delta_{a1} h_1$$

[illegible] $(e_{1k}, f_{1k}, e_{2k}, f_{2k})$.

$$[illegible] + f_{2k}\,B_{1k}) \,[illegible]_{mk}] - d_1\,D_m = 0$$

$$[illegible] (e_{1k}\,A_{2k} + f_{1k}\,[illegible] + e_{2k}\,[illegible] + f_{2k}\,[illegible]_{2k})\,\hat{D}_{mk}] - d_2\,\hat{D}_m = 0$$

$$[illegible]\,_{1k}\,A_{3k} + f_{1k}\,B_{3k}\,[illegible] + e_{2k}\,C_{3k} + f_{2k}\,D_{3k})\,\hat{D}_{mk}] - d_3\,D_m = 0$$

$$[illegible](e_{1k}\,A_{4k} + f_{1k}\,B_{4k})\,C_{mk} + (e_{2k}\,C_{4k} + f_{2k}\,D_{4k})\,C_{mk}] - d_4\,D_m = 0$$

$$m = 1,3,5\ldots 2N_k - 1$$

where

$$D_{mk} = \frac{1}{c}\int_{-c}^{c} \sin\,(\bar{\lambda}_{1m}\,x/c)\,\sin\,(\lambda_{1k}\,x/c)\,dx$$

$$\hat{D}_{mk} = \frac{1}{c}\int_{-c}^{c} \sin\,(\bar{\lambda}_{2m}\,x/c)\,\sin\,(\lambda_{2k}\,x/c)\,dx$$

$$C_{mk} = \frac{1}{c}\int_{-c}^{c} \sin\,(\bar{\lambda}_{1m}\,x/c)\,\sin\,(\lambda_{2k}x/c)\,dx$$

$$\bar{C}_{mk} = \frac{1}{c}\int_{-c}^{c} \sin\,(\bar{\lambda}_{2m}x/c)\,\sin\,(\lambda_{1k}x/c)\,dx = \bar{c}_{km}$$

$$D_m = \frac{1}{c^2}\int_{-c}^{c} x\,\sin\,(\bar{\lambda}_{1m}\,x/c)\,dx$$

$$[illegible] \int [illegible]$$

TABLE B4. VISCOUS RADIAL VELOCITY FUNCTIONS FOR CENTRAL ROD.

$$v_{1sv}(a,x) = \{h_1 x/c + \Sigma\, [E_{1k}\, h_{1k} + F_{1k}\, h_{2k}] \sin(\lambda_{1k} x/c)$$

$$+ \Sigma\, [E_{2k}\, h_{3k} + F_{2k}\, h_{4k}] \sin(\lambda_{2k} x/c)\}\, (c/a)\, \delta_{a1}\, \hat{K}$$

$$v_{2sv}(b_1,x) = \{h_2 x/c + \Sigma\, [E_{1k}\, h_{5k} + F_{1k}\, h_{6k}] \sin(\lambda_{1k} x/c)$$

$$+ \Sigma\, [E_{2k}\, h_{7k} + F_{2k}\, h_{8k}] \sin(\lambda_{2k} x/c)\}\, (c/b_1)\, \delta_{a2}\, \hat{K}$$

$$v_{2sv}(b_2,x) = \{h_1^* x/c + \Sigma\, [E_{1k}\, h_{1k}^* + F_{1k}\, h_{2k}^*] \sin(\lambda_{1k} x/c)$$

$$+ \Sigma\, [E_{2k}\, h_{3k}^* + F_{2k}\, h_{4k}^*] \sin(\lambda_{2k} x/c)\}\, (c/b_2)\, \delta_{a2}\, \hat{K}$$

$$h_1 = 2s\, [1 - 2\, \varepsilon_1^{\,2}\, (1 - N)\, \hat{D}^{-1}]\, (i - s)\, (i + s)^{-1}$$

$$h_2 = 4(\varepsilon_1 - \varepsilon_2)\, s\, (i - s)\, (i + s)^{-1}\, \hat{D}^{-1}$$

$$h_1^* = -2s\, [1 + 2\, \varepsilon_2^{\,2}\, (1 - N)\, \hat{D}^{-1}]\, (i - s)\, (i + s)^{-1}$$

$$h_{1k} = -[1 - 2\, \varepsilon_1^{\,2}\, (1 - N)\, \hat{D}^{-1}]\, \hat{f}_{1k}(a) + 2\, \varepsilon_1\, N\, \hat{D}^{-1}\, \hat{f}_{1k}(b_1)$$

$$h_{2k} = -[1 - 2\, \varepsilon_1^{\,2}\, (1 - N)\, \hat{D}^{-1}]\, \hat{g}_{1k}(a) + 2\, \varepsilon_1\, N\, \hat{D}^{-1}\, \hat{g}_{1k}(b_1)$$

$$h_{3k} = -2\, \varepsilon_1\, N\, \hat{D}^{-1}\, \hat{f}_{2k}(b_1)$$

$$h_{4k} = -2\, \varepsilon_1\, N\, \hat{D}^{-1}\, \hat{g}_{2k}(b_1)$$

$$h_{5k} = -2\, \varepsilon_1\, \hat{D}^{-1}\, \hat{f}_{1k}(a) + (1 + \varepsilon_1^{\,2} + \varepsilon_2^{\,2})\, \hat{D}^{-1}\, \hat{f}_{1k}(b_1)$$

TABLE B4. VISCOUS RADIAL VELOCITY FUNCTIONS FOR CENTRAL ROD (Continued).

$$h_{6k} = -2\ \varepsilon_1\ \hat{D}^{-1}\ \hat{g}_{1k}(d) + (1 + \varepsilon_1{}^2 + \varepsilon_2{}^2)\ \hat{D}^{-1}\ \hat{g}_{1k}(b_1)$$

$$h_{7k} = -(1 + \varepsilon_1{}^2 + \varepsilon_2{}^2)\ \hat{D}^{-1}\ \hat{f}_{2k}(b_1) + 2\ \varepsilon_2\ \hat{D}^{-1}\ \hat{f}_{2k}(b_2)$$

$$h_{8k} = -(1 + \varepsilon_1{}^2 + \varepsilon_2{}^2)\ \hat{D}^{-1}\ \hat{g}_{2k}(b_1) + 2\ \varepsilon_2\ \hat{D}^{-1}\ \hat{g}_{2k}(b_2)$$

$$h^*_{1k} = 2\ \varepsilon_2\ \hat{D}^{-1}\ \hat{f}_{1k}(b_1)$$

$$h^*_{2k} = 2\ \varepsilon_2\ \hat{D}^{-1}\ \hat{g}_{1k}(b_1)$$

$$h^*_{3k} = [1 + 2\ \varepsilon_2{}^2\ (1 - N)\ \hat{D}^{-1}]\ \hat{f}_{2k}(b_2) - 2\ \varepsilon_2\ \hat{D}^{-1}\ \hat{f}_{2k}(b_1)$$

$$h^*_{4k} = [1 + 2\ \varepsilon_2{}^2\ (1 - N)\ \hat{D}^{-1}]\ \hat{g}_{2k}(b_2) - 2\ \varepsilon_2\ \hat{D}^{-1}\ \hat{g}_{2k}(b_1)$$

APPENDIX C

AXISYMMETRIC EIGENVALUES

APPENDIX C. AXISYMMETRIC EIGENVALUES

The eigenvalues of this report were determined by linear perturbation functions whose azimuthal variation was exp $(-i\theta)$. A more general expression is exp $(-im\theta)$. Since the boundary conditions have an azimuthal variation corresponding to $m = 1$, the steady-state response required a consideration of this value of m only. Experimental measurements of eigenfrequencies have been made for axisymmetric waves $(m = 0)$ in a single liquid.[C1] In this appendix we will derive the equations for axisymmetric waves in two liquids.

The inviscid perturbation functions for any m have been derived in Reference C2. In Table C1 the appropriate expressions are given for $m \neq 1$. The more general definitions for δ_{aj} and δ_{cj}, also given in Reference C2, are

$$\delta_{ajm} = \frac{1 + i}{\sqrt{2(m+is)}} \, Re_j^{-1/2} \tag{C1}$$

$$\delta_{cjm} = -[2(m+is)]^{-1} \left[(2-m-is) \, \alpha_{jm}^{-1} - (2+m+is) \, \beta_{jm}^{-1} \right] \tag{C2}$$

$$\alpha_{jm} = (c/a) \, [s - (2+m) \, i]^{1/2} \, Re_j^{1/2} \tag{C3}$$

$$\beta_{jm} = (c/a) \, [s + (2-m) \, i]^{1/2} \, Re_j^{1/2}, \tag{C4}$$

where the complex roots are selected to have positive real parts.

Since velocities at rigid boundaries are zero for $m \neq 1$ perturbations, the corresponding viscous coefficient functions can be computed for an internal free surface from Table 2 when w_a, u_a, and v_a are defined to be

$$w_a = - w_{1si} \, (a,x). \tag{C5}$$

C1. [illegible], "Experimental Verification of the Inertia Oscillations of a [illegible] Cylinder [illegible] Spinup," BRL Contract Report 273, September [illegible] (See also Geophys. Astrophys. Fluid Dynamics, Vol. [illegible])

C2. [illegible], "[illegible] Liquid Payload During Spin-up Without a [illegible]," Ballistic Research Laboratory, Aberdeen Proving Ground, [illegible] Report ARBRL-TR-02581, August 1984. [illegible]

TABLE C1. INVISCID PERTURBATION FUNCTIONS FOR $m \neq 1$.

$$p_{jsi} = -(c/a)\ \Sigma\ R_{jkm}(r) \sin(\lambda_{km}\ x/c)\ \hat{K}$$

$$u_{jsi} = (s - im)^{-1}\ \Sigma\ R_{jkm}(r)\ \lambda_{km} \cos(\lambda_{km}\ x/c)\ \hat{K}$$

$$v_{jsi} = (c/a)\ \Sigma\ R_{vjkm}(r) \sin(\lambda_{km}\ x/c)\ \hat{K}$$

$$w_{jsi} = (c/a)\ \Sigma\ R_{wjkm}(r) \sin(\lambda_{km}\ x/c)\ \hat{K}$$

$$R_{jkm} = E_{jkm}\ J_m(\hat{\lambda}_{km}\ r/c) + F_{jkm}\ Y_m(\hat{\lambda}_{km}\ r/c)$$

$$R_{vjkm} = [(s - im)\ a\ R'_{jkm} - 2\ im\ (a/r)\ R_{jkm}]\ S_m^{-1}$$

$$R_{wjkm} = -[2\ a\ R'_{jkm} + im\ (s - im)\ (a/r)\ R_{jkm}]\ S_m^{-1}$$

$$\hat{\lambda}_{km}^2 = S_m \lambda_{km}^2\ (s - im)^{-2}$$

$$S_m = s^2 - 2\ ims + 4 - m^2$$

$$u_a = -u_{1si}\ (a,x) \tag{C6}$$

$$v_a = -\left[\frac{\partial(r\ v_{1si})}{\partial r}\right]_{r = a.} \tag{C7}$$

Table A1 can be used to compute viscous coefficient functions for a central rod and $m \neq 1$ if, in addition to Eqs. (C5-C7), similar definitions are assigned to w_b, u_b and v_b:

$$w_b = -w_{2si}\ (b_2,x) \tag{C8}$$

$$u_b = - u_{2si} (b_2, x) \tag{C9}$$

$$v_b = - \left[\frac{\partial (r\, v_{2si})}{\partial r} \right]_{r = b_2} . \tag{C10}$$

General versions of Eqs. (5.6-5.9) for $m \neq 1$ can now be derived

$$R_{1km}(b_1) - \rho_{21} R_{2km}(b_1) - (b_1/a) [R_{v1km}(b_1)$$
$$- \rho_{21} R_{v2km}(b_1)] (s - im)^{-1} = 0 \tag{C11}$$

$$R_{v1km}(b_1) - R_{v2km}(b_1) - (1 - \rho_{21}) \delta_{a2m} R^{\star}_{km} = 0 \tag{C12}$$

$$R_{2km}(b_2) - (b_2/a) (s - im)^{-1} R_{v2km}(b_2) = 0 \tag{C13}$$

$$R_{v1k}\ [illegible]\ \delta_{a1m} a R'_{v1km}(a) + \epsilon_1 N \delta_{a1m} R^{\star\star}_{km} D_0^{-1} = 0, \tag{C14}$$

where

$$R^{\star}_{km} [illegible] 1 + [illegible]_1^2 - [illegible]_2^2) a [R'_{v1km}(b_1) - R'_{v2km}(b_1)]$$
$$- 2 [illegible]_1 [illegible] b_1) [R_{v1km}(a) + a R'_{v1km}(a)]\} b_1^{-1}$$

$$R^{\star\star}_{km} [illegible] + b_1 R'_{v1km}(b_1) - R_{v2km}(b_1) - b_1 R'_{v2km}(b_1)] .$$

Eqs. (C11-C14) have been coded for m = 0 and eigenvalues can be computed. [illegible] axisymmetric eigenfrequency measurement for Re = 43,000 [illegible]. In Figure [illegible], [illegible] versus b_1/a is plotted for ρ_{21} = .4, .6, [illegible] value for a single liquid is plotted for b_1/a = 0, 1.

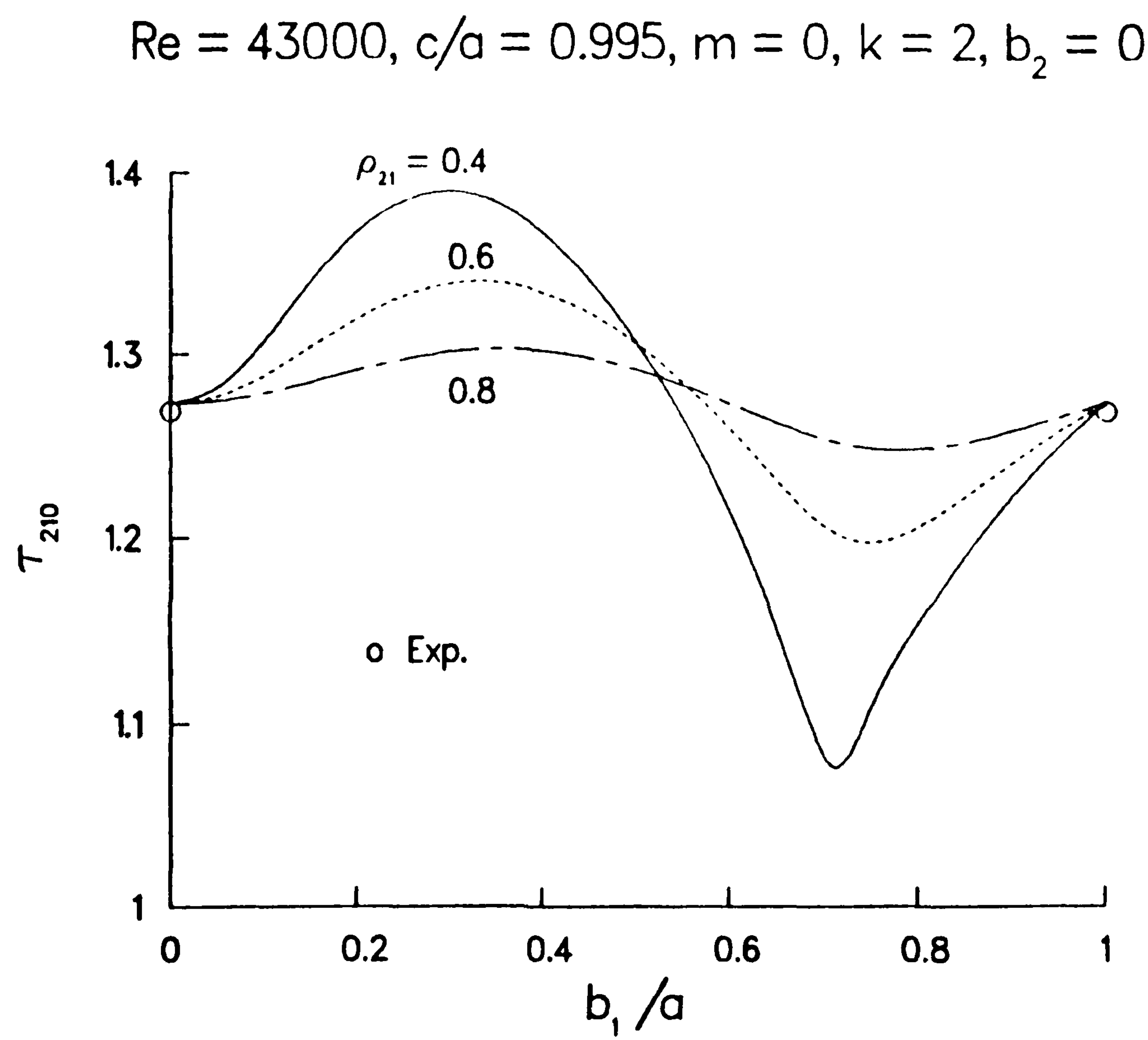

Figure C1. τ_{210} versus b_1/a for $Re_1 = 4.3 \times 10^4$, $c/a = 0.995$, $f = 1$, $m = 0$ and Various Density Ratios.

LIST OF SYMBOLS

a	radius of the cylindrical cavity containing the liquids
a_k	coefficients in a least squares fit of x/c to a series in sin (λ_k x/c), Eq. (5.5)
b_1	radius of the interface of the two liquids for $K_1 = 0$
b_2	radius of an air core (or central rod) for $K_1 = 0$
c	half-height of the cylindrical cavity containing the liquids
f	$1 - (b_2/a)^2$, the fill ratio
m_L	$2\pi\rho_1 a^2 c$, the liquid mass in the cavity fully filled with liquid 1
m_{pe}	pressure moment coefficient on the end walls, Eq. (6.5)
$m_{p\ell}$	pressure moment coefficient on the lateral wall, Eq. (6.4)
m_{pr}	pressure moment coefficient on the lateral wall, Eq. (A20)
m_{ve}	viscous moment coefficient on the end walls, Eq. (6.7)
$m_{v\ell}$	viscous moment coefficient on the lateral wall, Eq. (6.6)
m_{vr}	viscous moment coefficient on the lateral wall due to a rod, Eq. (A21)
p	liquid pressure
p_{js}	pressure perturbation in liquid j
p_{j} [illegible]	inviscid part of p_{js}

$\tilde{p}_{jsi}$	$p_{jsi} - (\tilde{r}\ \tilde{x}/a^2)\ \hat{K}$
p_{jsv}	viscous part of p_{js}
r	radial coordinate in the inertial system
$\tilde{r}$	radial coordinate in the aeroballistic system
s	$(\varepsilon + i)\tau$
s_{kn}	eigenvalues of s: the values of s that make the determinant of the system (5.6-5.9) zero
t	time
u_{jm}	coefficients in the expansion of u_{jsv}, Eqs. (4.6-4.7)
u_{js}, v_{js}, w_{js}	x, r, θ components of the liquid j velocity perturbation
u_{jsi}, v_{jsi}, w_{jsi}	inviscid part of u_{js}, v_{js}, w_{js}
u_{jsv}, v_{jsv}, w_{jsv}	viscous part of u_{js}, v_{js}, w_{js}
w_{jk}	coefficients in the expansion of w_{jsv}, Eqs. (4.4-4.5)
x	axial coordinate in the inertial system
$\tilde{x}$	axial coordinate in the aeroballistic system
C_{LIM}	liquid in-plane moment coefficient, defined by Eq. (6.1)
C_{LSM}	liquid side moment coefficient, defined by Eq. (6.1)
E_{jk}, F_{jk}	coefficients in the expression for R_{jk} computed by solving the system (5.6-5.9)

J_1	Bessel function of the first kind of order 1
$\hat{K}$	$K_1(0)\ e^{i\theta_1(0)}$
$K_1(t)$	amplitude of the coning motion
N	$\rho_{21}\ (\nu_2/\nu_1)^{1/2}$
N_k	number of terms considered in summing for $k = 1,3,5...(2\ N_k - 1)$
$M_{L\tilde{Y}}$, $M_{L\tilde{Z}}$	$\tilde{Y}$, $\tilde{Z}$ components of the liquid moment, Eq. (6.1)
Re_j	$a^2 \dot{\phi}^2 \nu_j^{-1}$, Reynolds number for liquid j
R_{jk}	$E_{jk}\ J_1\ (\hat{\lambda}_k r/c) + F_{jk}\ Y_1\ (\hat{\lambda}_k r/c)$
R_{vjk}	$[(s - i)\ a\ R'_{jk} - 2\ i\ (a/r)\ R_{jk}]\ S^{-1}$
R_{wjk}	$-[2\ a\ R'_{jk} + i\ (s - i)\ (a/r)\ R_{jk}]\ S^{-1}$
S	$s^2 - 2is + 3$
V_{xj}, V_{rj}, $V_{\theta j}$	x, r, θ components of the liquid j velocity, Eqs. (2.7-2.9)
XYZ	inertial system Cartesian axes, the X-axis tangent to the trajectory at time zero
$\tilde{X}\tilde{Y}\tilde{Z}$	aeroballistic system Cartesian axes, the $\tilde{X}$ -axis along the missile's axis of symmetry
Y_1	Bessel function of the second kind of order 1

$\tilde{\alpha}$ — angle of attack: the projection in the $\tilde{X}\tilde{Z}$ plane of the angle between the X and $\tilde{X}$ axes

$\tilde{\beta}$ — angle of sideslip: the projection in the $\tilde{X}\tilde{Y}$ plane of the angle between the X and $\tilde{X}$ axes

δ_{aj} — $\left[\dfrac{1 + i}{\sqrt{2}\,(1 + is)}\right] Re_j^{-1/2}$

δ_{cj} — $-\dfrac{(a/c)\ (1 + i)}{2\sqrt{2}\,(1 + is)}\left[\dfrac{1 - is}{\sqrt{3 + is}} + \dfrac{i(3 + is)}{\sqrt{1 - is}}\right] Re_j^{-1/2}$

Δp_i — fluctuating part of the inviscid pressure, Eq. (6.3)

ϵ — $(\dot{K}_1/K_1)\ \dot{\phi}_1^{-1}$, non-dimensionalized damping

ϵ_1 — $\exp\,[(b_1-a)/a\ \delta_{a1}]$

ϵ_2 — $\exp\,[(b_2-b_1)/a\ \delta_{a2}]$

η_j — dimensionless perturbation of liquid interfaces due to coning motion, Eqs. (2.5-2.6)

θ — azimuthal coordinate in the inertial system

$\tilde{\theta}$ — azimuthal coordinate in the aeroballistic system

Λ_k — "average" value of λ_{jk}, Eq. (3.5)

λ_{jk} — $(\pi k/2)\ (1 + \delta_{cj})$

$\hat{\lambda}_{jk}$ — $[S^{1/2}/(1 + is)]\ \lambda_{jk}$

μ_j	$\nu_j \rho_j$, dynamic viscosity of liquid j
ν_a	average kinematic viscosity, Eq. (3.5)
ν_j	kinematic viscosity of liquid j
ρ_j	density of liquid j
ρ_{21}	$\rho_2/\rho_1 \leq 1$
	$\dot{\phi}_1/\dot{\phi}$, nondimensionalized frequency
τ_{kn}	eigenfrequency for modes k and n; the imaginary part of s_{kn}
ϕ	$\dot{\phi}t$
$\dot{\phi}$	inertia spin rate
$\phi_1(t)$	phase angle of the coning motion

Derivatives:

$(\dot{\ })$	d( )/dt
$(\ )'$	d( )/dr

Indices:

e	endwall
j	liquid no. (1 heavier, 2 lighter)
k	axial mode number: 1,3,5,...(2 N_k - 1)
l	lateral wall
n	radial mode number: 1,2,3,...
p	pressure component
v	viscous (wall shear) component

DISTRIBUTION LIST

No. of Copies	Organization
12	Administrator Defense Technical Information Center ATTN: DTIC-DDA Cameron Station Alexandria, VA 22314
1	Commander US Army Materiel Command ATTN: AMCDRA-ST 5001 Eisenhower Avenue Alexandria, VA 22333
1	HQDA DAMA-ART-M Washington, DC 20310
1	Commander US Army Engineer Waterways Experiment Station ATTN: R.H. Malter P.O. Box 631 Vicksburg, MS 39180
1	Commander Armament R&D Center US Army AMCCOM ATTN: SMCAR-TDC Dover, NJ 07801
1	Commander Armament R&D Center US Army AMCCOM ATTN: SMCAR-TSS Dover, NJ 07801-5001
[illegible]	Commander Armament R&D Center US Army AMCCOM ATTN: SMCAR-LCA-F Mr. D. Mertz Mr. F. Falkowski Mr. A. Loeb Mr. R. Kline Mr. S. Kahn Mr. S. Wasserman Dover, NJ 07801-5001
1	Commander US Army Armament Munitions and Chemical Command ATTN: SMCAR-ESK-L Rock Island, IL 61299
1	Director Benet Weapons Laboratory Armament R&D Center US Army AMCCOM ATTN: SMCAR-LCB-TL Watervliet, NY 12189
1	Commander US Army Aviation Research and Development Command ATTN: AMSAV-E 4300 Goodfellow Blvd St. Louis, MO 63120
1	Director US Army Air Mobility Research and Development Laboratory ATTN: SAVDL-D, W.J. McCroskey Ames Research Center Moffett Field, CA 94035
1	Director US Army Air Mobility Research and Development Laboratory Ames Research Center Moffett Field, CA 94035
1	Commander US Army Communications Research and Development Command ATTN: AMSEL-ATDD Fort Monmouth, NJ 07703
1	Commander US Army Communications and Development Command ATTN: AMSEL-L Fort Monmouth, NJ 07703

PREVIOUS PAGE IS BLANK

DISTRIBUTION LIST

No. of Copies	Organization
1	Commander US Army Electronics Research and Development Command Technical Support Activity ATTN: AMDSD-L Fort Monmouth, NJ 07703
1	Commander US Army Missile Command ATTN: AMSMI-YDL Redstone Arsenal, AL 35898
1	Commander US Army Missile Command ATTN: AMSMI-R Redstone Arsenal, AL 35898
1	Commander US Army Missile Command ATTN: AMSMI-RDK, Mr. R. Deep Redstone Arsenal, AL 35898
1	Commander US Army Tank Automotive Command ATTN: AMSTA-TSL Warren, MI 48090
1	Director US Army TRADOC Systems Analysis Activity ATTN: ATAA-SL White Sands Missile Range, NM 88002
1	Commander US Army Jefferson Proving GD Madison, IN 47251
2	Commander US Army Research Office ATTN: Dr. R.E. Singleton Dr. Jagdish Chandra P.O. Box 12211 Research Triangle Park, NC 27709-2211
1	AGARD-NATO APO New York 09777
1	AFWL/SUL Kirtland AFB, NM 87117
1	Commandant US Army Infantry School ATTN: ATSH-CD-CSO-OR Fort Benning, GA 31905
3	Commander Naval Air Systems Command ATTN: AIR-604 Washington, DC 20360
2	Commander David W. Taylor Naval Ship Research & Development Cmd ATTN: H.J. Lugt, Code 1802 S. de los Santos Bethesda, MD 20084
1	Commander Naval Surface Weapons Center ATTN: DX-21, Lib Br Dahlgren, VA 22448
4	Commander Naval Surface Weapons Center Applied Aerodynamics Division ATTN: J.T. Frasier M. Ciment A.E. Winklemann W.C. Raysdale Silver Spring, MD 20910
1	AFATL (DLDL, Dr. D.C.Daniel) Eglin AFB, FL 32542
2	AFWAL (W.L. Hankey; J.S. Shang) Wright-Patterson AFB, OH 45433
1	Commander US Army Development & Employment Agency ATTN: MODE-TED-SAB Fort Lewis, WA 98433

DISTRIBUTION LIST

No. of Copies	Organization

[illegible]	Director
	National Aeronautics and Space
	  Administration
	Ames Research Center
	ATTN: W.C. Rose
	  B. Wick
	  P. Kutler
	  Tech Library
	Moffett Field, CA 94035

2	Director
	National Aeronautics and
	  Space Administration
	Langley Research Center
	ATTN: J. South
	  Tech Library
	Langley Station
	Hampton, VA 23365

1	Director National Aeronautics and Space Administration Lewis Research Center ATTN: MS 60-3, Tech Lib 21000 Brookpark Road Cleveland, OH 44135

[illegible]	Director
	National Aeronautics and
	  Space Administration
	Marshall Space Flight Center
	ATTN: A.R. Felix, Chief
	  S&E-AERO-AE
	  Dr. W.W. Fowlis
	[illegible]ville, AL 35812

1	[illegible] Systems Division ATTN: B. Reeves [illegible]well Street [illegible], MA 01887

[illegible]	[illegible] Research Org., Inc.
	ATTN: T.D. Whitfield
	  [illegible]. Matthews
	  [illegible]. Adams
	[illegible], TN 37389

3	Aerospace Corporation
	ATTN: H. Mirels
	  Walter F. Reddall
	  Aerophysics Lab.
	P.O. Box 92957
	Los Angeles, CA 90009

2	Director Jet Propulsion Laboratory ATTN: L.M. Mach Tech Library 4800 Oak Grove Drive Pasadena, CA 91109

3	Boeing Commercial Airplane
	  Company
	ATTN: R.A. Day, MS 1W-82
	  P.E. Rubbert, MS 3N-19
	  J.D. McLean, MS-3N-19
	Seattle, WA 98124

3	Calspan Corporation ATTN: G. Homicz P.O. Box 400 Buffalo, NY 14225
1	General Dynamics ATTN: Research Lib 2246 P.O. Box 748 Fort Worth, TX 76101
1	General Electric Company 3198 Chestnut Street Philadelphia, PA 19101
2	Grumman Aerospace Corporation ATTN: R.E. Melnik L.G. Kaufman Bethpage, NY 11714

2	Lockheed-Georgia Company
	ATTN: B.H. Little, Jr.
	  G.A. Pounds
	  Dept 72074, Zone 403
	86 South Cobb Drive
	Marietta, GA 30063

DISTRIBUTION LIST

No. of Copies	Organization
1	Lockheed Missiles and Space Company ATTN: Tech Info Center 3251 Hanover Street Palo Alto, CA 94304
3	Martin-Marietta Corporation ATTN: S.H. Maslen S.C. Traugott H. Obremski 1450 S. Rolling Road Baltimore, MD 21227
2	McDonnell Douglas Astronautics Corporation ATTN: J. Xerikos H. Tang 5301 Bolsa Avenue Huntington Beach, CA 92647
1	Douglas Aircraft Company ATTN: T. Cebeci 3855 Lakewood Boulevard Long Beach, CA 90846
3	Rockwell International Science Center ATTN: Dr. V. Shankar Dr. N. Malmuth Dr. S. Chakravarthy 1049 Camino Dos Rios Thousand Oaks, CA 91360
4	Director Sandia National Laboratory ATTN: H.W. Vaughn G. Wolfe W.L. Oberkampf Tech Lib. Albuquerque, NM 87115
2	United Aircraft Corporation Research Laboratory ATTN: M.J. Werle Library 400 Main Street East Hartford, CT 06108

No. of Copies	Organization
1	Vought Corporation ATTN: J.M. Cooksey, Chief, Gas Dynamics Lab, 2-53700 P.O. Box 5907 Dallas, TX 75222
2	Arizona State University Department of Mechanical and Energy Systems Engineering ATTN: G.P. Neitzel W.S. Saric Tempe, AZ 85287
1	Cornell University Graduate School of Aero Engr ATTN: Library Ithaca, NY 14853
3	California Institute of Technology ATTN: Tech Library H.B. Keller, Math Dept D. Coles, Aero Dept Pasadena, CA 91109
1	Illinois Institute of Tech ATTN: S. Rosenblat 3300 South Federal Chicago, IL 60616
1	The Johns Hopkins University Dept of Mech and Materials Sci. ATTN: S. Corrsin Baltimore, MD 21218
1	Louisiana State University Dept. of Physics and Astronomy ATTN: Dr. R.G. Hussey Baton Rouge, LA 70803
3	Massachusetts Institute of Technology ATTN: E. Covert H. Greenspan Tech Lib 77 Massachusetts Avenue Cambridge, MA 02139

DISTRIBUTION LIST

No. of Copies	Organization
4	Director Johns Hopkins University Applied Physics Laboratory ATTN: Dr. R.D. Whiting Dr. D.A. Hurdif Dr. R.S. Hirsh Mr. E.R. Bohn Johns Hopkins Road Laurel, MD 20707
2	North Carolina State Univ Mechanical and Aerospace Engineering Department ATTN: F.F. DeJarnette J.C. Williams Raleigh, NC 27607
1	Northwestern University Department of Engineering Science and Applied Mathematics ATTN: Dr. S.H. Davis Evanston, IL 60201
1	Notre Dame University Department of Aero Engr ATTN: T.J. Mueller Notre Dame, IN 46556
2	Ohio State University Dept of Aeronautical and Astronautical Engineering ATTN: S.L. Petrie O.R. Burggraf Columbus, OH 43210
1	Purdue University Thermal Science & Prop Ctr ATTN: Tech Library W. Lafayette, IN 47906
2	Polytechnic Institute of New York ATTN: G. Moretti Tech Library Route 110 Farmingdale, NY 11735
3	Princeton University James Forrestal Research Ctr Gas Dynamics Laboratory ATTN: S.M. Bogdonoff S.I. Cheng Tech Library Princeton, NJ 08540
1	Rensselaer Polytechnic Institute Department of Math Sciences ATTN: Tech Library Troy, NY 12181
1	Rutgers University Department of Mechanical, Industrial, and Aerospace Engineering ATTN: R.H. Page New Brunswick, NJ 08903
1	San Diego State University Department of Aerospace Engr and Engineering Mechanics College of Engineering ATTN: K.C. Wang San Diego, CA 92115
1	Southern Methodist University Department of Civil and Mechanical Engineering ATTN: R.L. Simpson Dallas, TX 75222
1	Southwest Research Institute Applied Mechanics Reviews 8500 Culebra Road San Antonio, TX 78228
2	Stanford University Dept of Aeronautics/Astronautics ATTN: J.L. Steger M. Van Dyke Stanford, CA 94305

DISTRIBUTION LIST

No. of Copies	Organization
1	Texas A&M University College of Engineering ATTN: R.H. Page College Station, TX 77843
1	University of California - Davis ATTN: H.A. Dwyer Davis, CA 95616
1	University of California - Berkeley Department of Aerospace Engineering ATTN: M. Holt Berkeley, CA 94720
2	University of California - San Diego Department of Aerospace Engineering and Mechanical Engineering Sciences ATTN: P. Libby Tech Library La Jolla, CA 92037
1	University of California - Santa Barbara Department of Mechnical and Environmental Engineering ATTN: J.P. Vanyo Santa Barbara, CA 93106
1	University of Colorado Department of Astro-Geophysics ATTN: E.R. Benton Boulder, CO 80302
2	University of Cincinnati Department of Aerospace Engineering ATTN: R.T. Davis S.G. Rubin Cincinnati, OH 45221
2	University of Maryland ATTN: W. Melnik J.D. Anderson College Park, MD 20740
1	University of Maryland - Baltimore County Department of Mathematics ATTN: Dr. Y.M. Lynn 5401 Wilkens Avenue Baltimore, MD 21228
1	University of Santa Clara Department of Physics ATTN: R. Greeley Santa Clara, CA 95053
2	University of Southern California Department of Aerospace Engineering ATTN: T. Maxworthy P. Weidman 3551 University Ave Los Angeles, CA 90007
2	University of Michigan Department of Aeronautical Engineering ATTN: W.W. Wilmarth Tech Library East Engineering Building Ann Arbor, MI 48104
2	University of Rochester Department of Mechanical and Aerospace Sciences ATTN: R. Gans A. Clark, Jr. Rochester, NY 14627
1	University of Tennessee Department of Physics ATTN: Prof. W.E. Scott Knoxville, TN 37916

DISTRIBUTION LIST

No. of Copies	Organization
1	University of Texas Department of Aerospace Engineering ATTN: J.C. Westkaemper Austin, TX 78712
3	University of Virginia Department of Mechanical Aerospace Engineering ATTN: W.G. Wood R.J. Ribando R. Krauss Charlottesville, VA 22904
1	University of Washington Department of Mechanical Engineering ATTN: Tech Library Seattle, WA 98105
1	University of Wyoming ATTN: D.L. Boyer University Station Laramie, WY 82071
1	U.S. Military Academy Department of Physics ATTN: MAJ G. Heuser West Point, NY 10996
1	University of Wisconsin - Madison Mathematics Research Center ATTN: John C. Strikwerda 610 Walnut Street Madison, Wisconsin 53705

No. of Copies	Organization
1	Woods Hole Oceanographic Institute ATTN: J.A. Whitehead Woods Hole, MA 02543
2	Virginia Polytechnic Institute and State University Department of Aerospace Engineering ATTN: Tech Library Dr. T. Herbert Blacksburg, VA 24061

Aberdeen Proving Ground

Director, USAMSAA
ATTN: AMXSY-D
AMXSY-MP, H. Cohen

Commander, USATECOM
ATTN: AMSTE-TO-F

Commander, CRDC, AMCCOM
ATTN: SMCCR-RSP-A
W. C. Dee
SMCCR-MU
M. C. Miller
ATTN: SMCCR-RSP-A
SMCCR-MU
SMCCR-SPS-IL

USER EVALUATION SHEET/CHANGE OF ADDRESS

This Laboratory undertakes a continuing effort to improve the quality of the reports it publishes. Your comments/answers to the items/questions below will aid us in our efforts.

1. BRL Report Number_______________ Date of Report ________

2. Date Report Received_______________

3. Does this report satisfy a need? (Comment on purpose, related project, or other area of interest for which the report will be used.)_______________

4. How specifically, is the report being used? (Information source, design data, procedure, source of ideas, etc.)_______________

5. Has the information in this report led to any quantitative savings as far as man-hours or dollars saved, operating costs avoided or efficiencies achieved etc? If so, please elaborate._______________

6. General Comments. What do you think should be changed to improve future reports? (Indicate changes to organization, technical content, format, etc.)

CURRENT ADDRESS

Name

Organization

Address

City, State, Zip

7. If indicating a Change of Address or Address Correction, please provide the New or Correct Address in Block 6 above and the Old or Incorrect address below.

OLD ADDRESS

Name

Organization

Address

City, State, Zip

(Remove this sheet along the perforation, fold as indicated, staple or tape closed, and mail.)

FOLD HERE

Director
US Army Ballistic Research Laboratory
ATTN: AMXBR-OD-ST
Aberdeen Proving Ground, MD 21005-5066

NO POSTAGE
NECESSARY
IF MAILED
IN THE
UNITED STATES

OFFICIAL BUSINESS
PENALTY FOR PRIVATE USE, $300

BUSINESS REPLY MAIL
FIRST CLASS PERMIT NO 12062 WASHINGTON, DC

POSTAGE WILL BE PAID BY DEPARTMENT OF THE ARMY

Director
US Army Ballistic Research Laboratory
ATTN: AMXBR-OD-ST
Aberdeen Proving Ground, MD 21005-9989

FOLD HERE

END

FILMED

2-85

DTIC